Prostate Imaging for Recurrence Reporting: User Guide

Anup S. Shetty, MD • Tyler J. Fraum, MD • Joseph E. Ippolito, MD, PhD • Mohamed Z. Rajput, MD • Mark J. Hoegger, MD, PhD • David H. Ballard, MD
Richard Tsai, MD • Cary L. Siegel, MD • Chelsea Schmitt, MD, MPH • Syed MA Shah, MD • Daniel R. Ludwig, MD

Author affiliations, funding, and conflicts of interest are listed at the end of this article.
See the invited commentary by Dias and Haider in this issue.

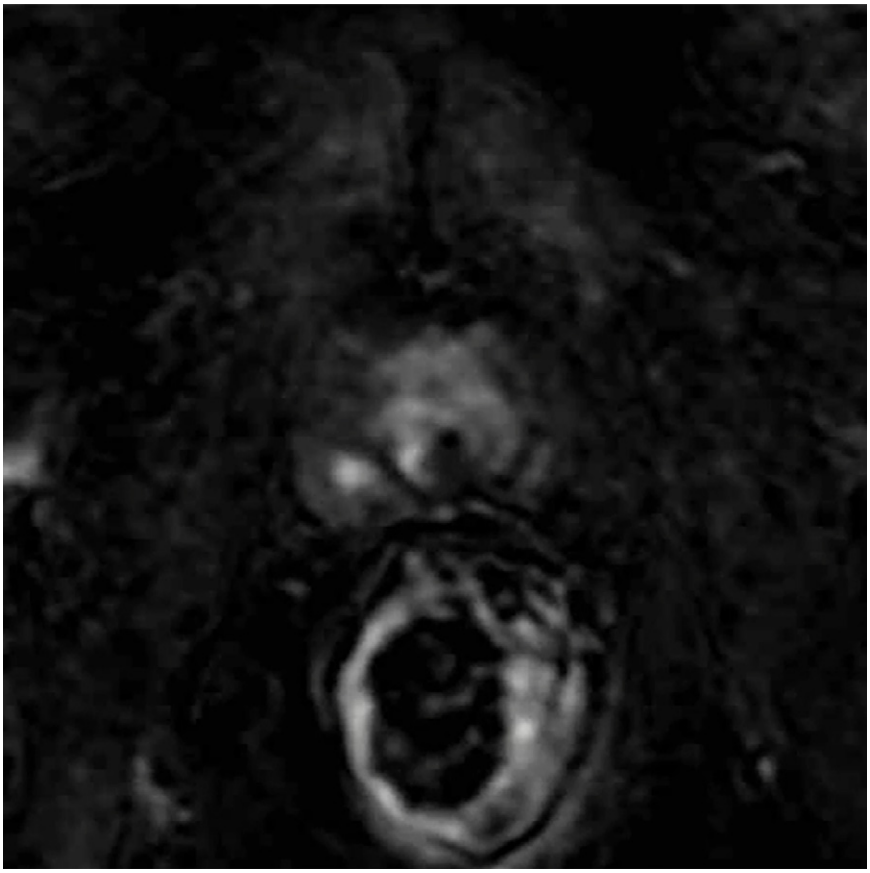

The Prostate Imaging for Recurrence Reporting (PI-RR) system was introduced in 2021 to standardize the performance and interpretation of pelvic MRI after whole-gland treatment with radical prostatectomy (RP) or radiation therapy (RT). The Prostate Imaging Reporting and Data System (PI-RADS) defines technical and reporting standards for imaging prostate cancer before treatment. Although similar imaging techniques can be applied in assessing the treated prostate gland, the interpretation varies substantially between PI-RADS and PI-RR. With PI-RADS, T2-weighted and diffusion-weighted imaging are emphasized for cancer detection. After treatment, the emphasis shifts in PI-RR to detect recurrence with dynamic contrast enhancement (DCE) imaging. Focal early enhancement on DCE images, and to a lesser degree marked diffusion restriction, are the key MRI findings of recurrence after RP and RT. Using nomenclature similar to that of PI-RADS version 2.1, PI-RR uses established knowledge of recurrent prostate cancer MRI features and systematically codifies scoring elements. The authors discuss the PI-RR rationale, technical standards, and reporting guidelines. The scoring system for posttreatment MRI after RT and RP is reviewed, exploring the relevant T2-weighted, diffusion-weighted, and DCE features for both scenarios. The use of PI-RR is illustrated through instructive cases. Finally, pitfalls in the initial implementation of PI-RR and areas for future development are described. The goal is to provide a comprehensive reference for prostate MRI readers of all experience levels to use PI-RR in standardizing reporting of suspected recurrent prostate cancer.

©RSNA, 2025 • *radiographics.rsna.org*

Introduction

Prostate cancer remains the most common new noncutaneous cancer diagnosis in American men, with nearly 300 000 new cases and 35 000 deaths in 2024 (1). In patients with localized, potentially curable prostate cancer and good performance status, whole-gland therapies such as radical prostatectomy (RP) or external beam radiation therapy (RT) are the primary treatment modalities (2). Biochemical recurrence (BCR) is defined by a prostate-specific antigen (PSA) level of greater than or equal to 0.2 ng/mL on two consecutive measurements after RP or an increase of 2 ng/mL above nadir after RT (3). In the case of BCR following these curative-intent strategies, distinguishing between local and systemic recurrence is crucial in guiding decisions regarding local salvage therapy (4). Detection of local recurrence after RT is especially important owing to the morbidity of local salvage treatments,

An earlier incorrect version of this article appeared online. This article was corrected on August 1, 2025.

This copy is for personal use only. To order copies, contact *reprints@rsna.org*.

Invited Commentary TestYour Knowledge CME

RadioGraphics 2025; 45(8):e240145
https://doi.org/10.1148/rg.240145

Content Codes: GU, MR, NM

Abbreviations: BCR = biochemical recurrence, DCE = dynamic contrast enhanced, DWI = diffusion-weighted imaging, FOV = field of view, PI-RADS = Prostate Imaging Reporting and Data System, PI-RR = Prostate Imaging for Recurrence Reporting, PSA = prostate-specific antigen, PSMA = prostate-specific membrane antigen, PZ = peripheral zone, RP = radical prostatectomy, RT = radiation therapy, TZ = transitional zone, VUA = vesicourethral anastomosis

TEACHING POINTS

- The Prostate Imaging for Recurrence Reporting (PI-RR) scheme was introduced in 2021 in an effort to formalize the performance and interpretation of pelvic MRI for the assessment of local recurrence after RP and RT.
- Whether assessing the post-RP or post-RT pelvis, subtraction imaging for DCE acquisitions helps increase the conspicuity of early enhancement of suspicious lesions.
- Most local recurrences after RT occur at the site of the primary tumor, with less than 10% occurring elsewhere.
- DWI and DCE are considered codominant sequences for PI-RR scoring after RT, with the higher of either score resulting in the final PI-RR characterization.
- The VUA and perianastomotic region is the most common site of local recurrence after RP. Other potential sites include the rectovesical space, seminal vesicles, pelvic floor abutting the levator ani muscles, and, less commonly, the penis.

most commonly RP (5). On the other hand, salvage RT is often indicated after RP in patients with BCR if there is no evidence of distant metastases (6). Many patients with BCR have lesions that are too small for effective biopsy (particularly after RP), leaving PSA levels and imaging findings as the primary determinants of additional therapy.

Although pelvic MRI has been performed for at least the past 25 years to assess for local recurrence (7), standardized guidelines have been lacking. The Prostate Imaging for Recurrence Reporting (PI-RR) scheme was introduced in 2021 in an effort to formalize the performance and interpretation of pelvic MRI for the assessment of local recurrence after RP and RT (4). This article provides the background and rationale for PI-RR, data supporting its use, MRI protocol considerations, and a detailed discussion of the scoring system, including case examples, and pitfalls in interpretation.

Background

Rationale

In patients with BCR, MRI is preferred over CT for pelvic staging, and its use is recommended in addition to prostate-specific membrane antigen (PSMA) PET in the setting of recurrence after RT (3,6,8). MRI may not be typically included in the initial workup for patients with BCR after RP. Further evaluation and treatment may be considered for patients with suspected recurrence if their life expectancy is greater than 5 years. The PSA doubling time (PSADT) can be helpful in assessing the likelihood of local versus systemic recurrence. Patients with a long PSADT are more likely to have local recurrence, whereas those with a short PSADT are more likely to have systemic recurrence (9).

The Prostate Imaging Reporting and Data System (PI-RADS) version 2.1 (PI-RADS 2.1) has been extensively validated for the detection and risk stratification of prostate cancer (10). However, PI-RADS is applicable only to the treatment-naive prostate gland (11). After RT, the prostate becomes atrophic and diffusely T2 hypointense, often with loss of anatomic delineation between the peripheral zone (PZ) and transitional zone (TZ) (12). T2-weighted imaging after RT remains useful for anatomic localization and comparison with pretreatment imaging but has limited utility for the detection of recurrence. Postoperative changes after RP such as fibrosis, hematoma, and residual prostate tissue similarly limit the utility of T2-weighted imaging after RP.

Recurrent prostate cancer after definitive treatment has a high degree of vascularity, especially relative to fibrosis with the prostate gland following RT or to residual prostate tissue in the operative bed after RP (13,14). Therefore, T1-weighted dynamic contrast-enhanced (DCE) imaging becomes a primary imaging sequence in detecting recurrence after treatment, which typically appears as focal or masslike early enhancement and stands out against the delayed enhancement of fibrotic tissue. In contradistinction, for PI-RADS 2.1, DCE imaging serves only an ancillary role as a tie-breaking feature in the PZ and has no role in evaluation of the TZ (11).

Diffusion-weighted imaging (DWI) also has an important role in detecting recurrence after treatment owing to the high cellular density of recurrent tumors. However, the sensitivity of DWI to signal loss from susceptibility limits its utility when assessing tissue near brachytherapy seeds, fiducial markers, and surgical clips, especially when the size of the recurrence is small (15). Despite these considerations, pelvic MRI has excellent overall performance and is considered the modality of choice for detecting local recurrence after RT and RP (16–18). Furthermore, concordant findings at DCE imaging and DWI increase the confidence in the determination of local recurrence, as reflected in PI-RR.

12/28/2025

Development of PI-RR

Before the introduction of PI-RR, there was no established guidance or standardization for detecting or reporting local recurrence after RT or RP using pelvic MRI. Previous systematic reviews showed pooled sensitivity using MRI as high as 84%, although this was dependent on the PSA level at the time of imaging (16,19). PI-RR was introduced in 2021 to address this gap in clinical practice (4). PI-RR leverages knowledge of MRI features of recurrent prostate cancer and systematically provides a scoring and reporting framework to determine the likelihood of recurrent prostate cancer. These guidelines were based on a nonsystematic review of available literature in consensus by members of the European Society of Urogenital Radiology, the European Society of Urologic Imaging, and the PI-RADS steering committee. Although data supporting the use of PI-RR is limited to date and it has not been formally endorsed at this time by the societies that the authors represent, standardized reporting has high potential value, not

Table 1: Available Evidence for PI-RR

Study* and Treatment Type	No. of patients	Sensitivity (%)	Specificity (%)	Positive Predictive Value (%)	Negative Predictive Value (%)	Accuracy (%)	Interobserver Agreement (k)	Local detection rate (MRI vs choline PET/CT)	Local detection rate (MRI vs PSMA PET/CT)
Pecoraro et al (20)									
Radiation	48	71–81	74–93	71–89	79–86	77–88	0.87 (95% CI: 0.81, 0.93)	…	…
Prostatectomy	52	59–83	87–100	88–100	66–80	75–85	0.87 (95% CI: 0.80, 0.92)	…	…
Bergaglio et al (21)									
Prostatectomy or radiation	76	68–71	82–90	79–87	72–76	75–80	0.74 (95% CI: 0.62–0.87)	…	…
Ciccarese et al (22)									
Prostatectomy	134	85	33	73	50	68	0.88 ($P <$ 0.001)	70% vs 20%	59% vs 23%
Franco et al (23)									
Prostatectomy or radiation	120	79–86	64–86	95–98	33–46	79–87	(0.52–0.77)	…	…

* Numbers in parentheses in this column denote reference numbers.

only for clinical practice but also for clinical research and data collection. Additional iterations of PI-RR are a near certainty after additional validation studies are performed.

Available Evidence for PI-RR

Given the recent introduction of PI-RR in 2021, supporting data are limited, derived from only a few retrospective analyses (Table 1). A challenge in clinical research studies to guide management of patients with BCR is the inconsistent availability of histologic correlation, with reference standards that may include biopsy, imaging findings, clinical follow-up, or a combination thereof. A PI-RR score of 3 or greater has strong performance for detection of recurrence with an overall accuracy of 68%–88% across studies. PI-RR also has been shown to have excellent reproducibility across readers.

In a retrospective study with four experienced readers, Pecoraro et al (20) showed in a cohort of 100 men with an average PSA level of approximately 7.3 ng/mL that a PI-RR score of 3 or greater yielded high specificity and positive predictive value with excellent interobserver agreement in patients who underwent RT and those who underwent RP. Bergaglio et al (21) showed similar results in a retrospective three-reader study (with two radiologists and a radiology resident) of 76 men treated predominantly with RP, with substantial interreader agreement. In a retrospective two-reader study of 134 men who underwent treatment with RP, Ciccarese et al (22) showed a lower accuracy, specificity, and positive predictive value than did Pecoraro et al (20) and Bergaglio et al (21) but found excellent interobserver agreement. Ciccarese et al (22) also showed a positive correlation between PI-RR scores and serum PSA levels and found a better local detection rate for MRI compared with that for choline PET/CT (70% vs 20%, respectively) and PSMA PET/CT (59% vs 23%, respectively).

In a retrospective study with five readers of variable experience levels, Franco et al (23) published similar findings of high sensitivity and positive predictive value in a cohort of 120 men who underwent treatment with either RP or RT, although with only good to excellent interobserver agreement. Akkaya et al (24) specifically assessed factors influencing interobserver agreement with PI-RR scoring and found better agreement with a PSA level greater than 0.5 ng/mL and recurrent tumor size greater than 1 cm. Park et al (13) evaluated the concordance of DCE findings at a positive surgical margin within a year of RP with higher Gleason score and PSA level and found that 73% of sites of focal nodular enhancement were concordant with the site of positive surgical margin. Kim et al (25) found an overall accuracy of 48% with positive and negative predictive values of 85% and 38%, respectively, and sensitivity and specificity of 27% and 90%, respectively, in their retrospective analysis. Data from select PI-RR retrospective series are summarized in Table 1.

Imaging Protocol

Technical Standards

PI-RR follows the technical standards of multiparametric small field-of-view (FOV) T2-weighted imaging, DWI, and DCE imaging outlined in PI-RADS 2.1 (Table 2) (4). A 3-T field strength is preferred to 1.5 T unless patients have metallic devices or implants, per a recent review on prostate imaging quality (26). Although biparametric MRI has gained attention for use in PI-RADS (27), this technique is not suitable for use in PI-RR to assess for recurrent prostate cancer due to the primacy of DCE imaging in assessing for recurrence. Small FOV T2-weighted imaging, which is expanded from the PI-RADS requirement of axial plus either coronal or sagittal plane imaging to triplanar imaging, should include the structures where recurrence commonly occurs, including the entire posterior urinary bladder wall, vesicourethral anastomosis (VUA), and any residual seminal vesicle tissue. Full FOV imaging of the pelvis, either T1-weighted or diffusion weighted, is performed to assess for metastases in the bones

Table 2: Sample Protocol for PI-RR Pelvic MRI

Sequence Name	ST (mm)	Matrix (pixels)	TR (msec)	TE (msec)	NSA	FOV (mm)	TA (min:sec)	Notes
T2W single-shot FSE coronal	6	320 × 320	1500	100	1	300 × 380	0:45	Whole pelvis coverage
T2W FSE axial small FOV	3	512 × 512	8500	105	2	160 × 160	3:00	Cover entire posterior wall of bladder and seminal vesicles
T2W FSE coronal small FOV	3	512 × 512	8500	105	2	160 × 160	3:00	Cover entire posterior wall of bladder and seminal vesicles
T2W FSE sagittal small FOV	3	512 × 512	8500	105	2	160 × 160	3:00	Cover entire posterior wall of bladder and seminal vesicles
DWI single-shot axial small FOV	3	228 × 228	5400	72	2, 10	200 × 200	5:20	Obtain *b* values of 50 and 800 sec/mm²; reconstruct ADC map and calculated high *b* value of 1400 sec/mm²
DWI multishot readout segmented small FOV	3	236 × 236	6000	75	4	200 × 200	3:30	Obtain single *b* value of 2000 sec/mm²
DWI single-shot axial full FOV	6	256 × 328	7800	56	4, 7, 10	300 × 380	3:20	Whole pelvis coverage Obtain *b* values of 50, 400, and 800 sec/mm²; reconstruct ADC map
T1W 3D spoiled GRE Dixon axial precontrast full FOV	3	280 × 352	5.51	2.46	1	300 × 380	1:07	Acquire in-phase and opposed-phase, additionally reconstruct fat-only and water-only
T1W 3D spoiled GRE DCE small FOV	3	320 × 320	4.84	1.77	1	200 × 200	2:50	Acquire 20 consecutive phases with temporal resolution per phase <10 sec; inject contrast material at start of third phase; either generate subtraction images using the first phase as a mask on the scanner or in software
T1W 3D spoiled GRE Dixon axial postcontrast full FOV	3	280 × 352	5.51	2.46	1	300 × 380	1:07	Acquire in-phase and opposed-phase, additionally reconstruct fat-only and water-only; generate automated subtraction images

Note.—Scan time is approximately 35–40 minutes. ADC = apparent diffusion coefficient, FSE = fast spin echo, GRE = gradient-recalled echo, NSA = number of signal averages, ST = section thickness, TA = acquisition time, TE = echo time, T1W = T1-weighted, T2W = T2-weighted, TR = repetition time, 3D = three-dimensional.

and lymph nodes. The authors include full FOV imaging on all prostate MRI examinations to meet technical standards of PI-RR regardless of whether the patient has undergone definitive treatment, as the treatment history may not be known at the time of protocoling the examination. Bowel preparation is not specifically addressed by PI-RADS 2.1 or PI-RR, and techniques such as enema, rectal catheter to evacuate gas, dietary restriction, and antiperistaltic medications lack strong evidence but can be considered for use (26).

Additional Protocol Considerations

In addition to full FOV DWI, the authors perform full FOV T1-weighted imaging with an axial three-dimensional spoiled gradient-echo Dixon technique in which a precontrast breath-hold acquisition generates in-phase, opposed-phase, fat-only, and water-only images (Table 2) (28). The fat-only reconstruction provides a rapid method for screening for bone metastases, which will be dark compared with normally high- or intermediate-signal-intensity fat-containing marrow. In-phase and opposed-phase source data can also be used to assess the percentage of signal intensity decrease between the two, using the following formula:

$$\%\ \text{chemical shift signal loss} = 100 \times \frac{\text{In phase signal intensity} - \text{Opposed phase signal intensity}}{\text{In phase signal intensity}}$$

Chemical shift signal intensity loss greater than 20% indicates a higher likelihood of benignity (ie, a sufficient proportion of fat indicating normal bone marrow) (29). After DCE imaging is performed, a repeat Dixon acquisition is acquired, and automated water-only subtractions are generated, facilitating detection of enhancing bone lesions with greater conspicuity.

Whether assessing the post-RP or post-RT pelvis, subtraction imaging for DCE acquisitions helps increase the conspicuity of early enhancement of suspicious lesions (Fig 1) (30). Subtracted DCE images can either be generated on the scanner itself, particularly if a study is to be reviewed in a standard picture archiving and communication system (PACS) system, or can be generated with software platforms that are

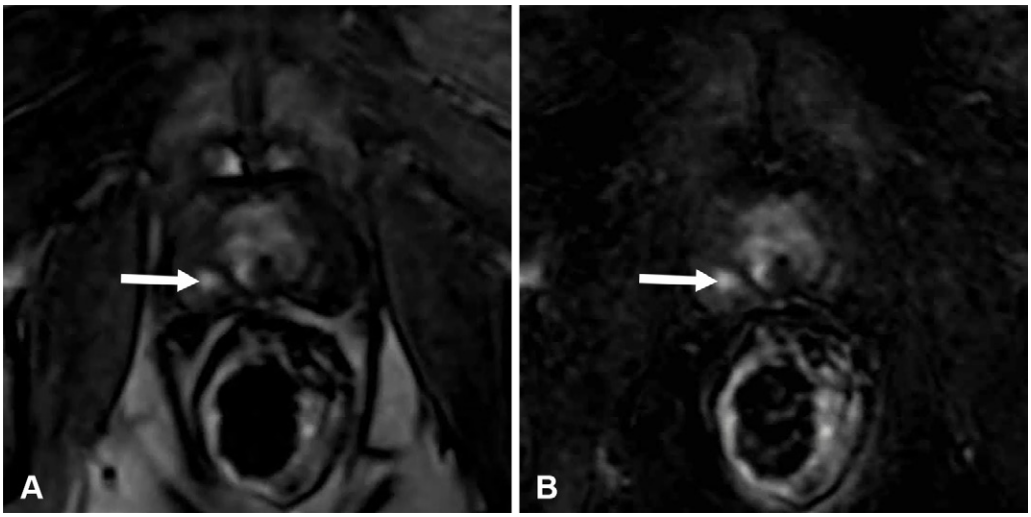

Figure 1. Subtraction imaging for DCE acquisition in a 64-year-old man with prostate cancer (Gleason score 3 + 4) treated with external beam RT 4 years prior with a rising PSA level of 2 ng/mL. **(A)** Axial T1-weighted DCE MR image shows a focus of early enhancement in the right PZ (arrow). **(B)** Axial T1-weighted DCE MR image using subtraction (with the first time point in **A** as the mask) shows better background signal suppression and improved conspicuity of a site of disease recurrence (arrow).

frequently used for prostate MRI interpretation. In the authors' practice, contrast material injection occurs after the second dynamic time point acquisition. The first time point, at which no intravenous contrast material is present, is used as the mask for generating subtractions of each of the subsequent DCE imaging time points. Subtraction DCE imaging may be preferable to fat-suppressed DCE imaging, which can be compromised by loss of background soft-tissue anatomic detail from susceptibility artifacts from metal, such as implanted seeds or fiducial markers. Motion-correction algorithms can be applied to the DCE dataset to account for involuntary prostate motion due to the passage of rectal gas during the minutes-long acquisition (31). Given the greater reliance of PI-RR than PI-RADS 2.1 at DCE imaging, the optimization of DCE imaging is highly recommended.

In patients with metallic implants such as hip arthroplasties or instrumentation, metal artifact reduction (MAR) techniques can improve image quality and diagnostic confidence. Options for mitigating susceptibility artifacts include imaging at a lower magnetic field strength (1.5 T rather than 3.0 T) and/or using sequences designed to reduce these artifacts. The authors image with 3.0 T using MAR techniques, with the rationale that the improved signal-to-noise ratio provides a greater benefit than the drawback of susceptibility, particularly when using MAR techniques. MAR options include high bandwidth view-angle tilting for two-dimensional T2-weighted imaging, small FOV selective excitation zoomed single-shot echo-planar DWI, and readout-segmented multishot echo-planar DWI (28). Compared with standard techniques, MAR techniques frequently require longer acquisition times and have lower signal-to-noise ratio and/or blurring. Technologists should be encouraged to use these techniques not only when hip instrumentation is encountered but also for surgical clips, fiducial markers, or brachytherapy seeds that commonly result in susceptibility artifacts.

Scoring System

The PI-RR scoring system, like PI-RADS 2.1, uses a 1–5 Likert scale representing the likelihood of recurrent prostate cancer, with 1 corresponding to a very low likelihood and 5 corresponding to a very high likelihood (4). The scoring systems differ between the treatment modalities for RP and RT and are detailed in the following sections. Importantly, PI-RR takes into account the location (in the case of RT) or side (in the case of RP) of the primary tumor at initial staging. Thus, interpretation benefits greatly from access to prior imaging and pathology data.

Radiation Therapy

Most local recurrences after RT occur at the site of the primary tumor, with less than 10% occurring elsewhere (32). Imaging should occur at least 3 months after completion of RT to avoid confounding early enhancement with DCE imaging from treatment-related inflammation (33). T2-weighted imaging is helpful for anatomic localization but limited in detecting recurrence due to the typically diffuse T2-weighted intermediate-to-low signal intensity representing posttreatment fibrosis (Fig 2) (34). DCE and DWI are thus the primary features assessed (Fig 3). There is no distinction between PZ and TZ recurrence in the PI-RR system. Brachytherapy seeds and fiducial markers can create susceptibility artifacts, and thus one must integrate data from all sequences in arriving at a PI-RR classification.

Typical recurrences after RT resemble de novo prostate cancer, with focal T2-weighted hypointensity, DWI hyperintensity and apparent diffusion coefficient (ADC) hypointensity, and early enhancement at DCE imaging (Figs 4–6) (35). The treated prostate gland after RT is frequently atrophic with diffuse T2-weighted intermediate-to-hypointense signal intensity and loss of normal zonal anatomic distinction between the PZ and TZ (Fig 2). Although a T2-weighted score is assigned to focal abnormalities in a similar fashion as those in PI-RADS 2.1 (Fig 4), the score plays no role in determining the PI-RR characterization. T2-weighted imaging is primarily helpful in anatomic localization and comparison with pretreatment imaging when available.

DWI scoring in PI-RR follows a similar pattern as scoring in PI-RADS 2.1, although rather than designating a score of 2 corresponding to linear- or wedge-shaped abnormal ADC or DWI signal intensity as in PI-RADS 2.1, a diffuse moderate

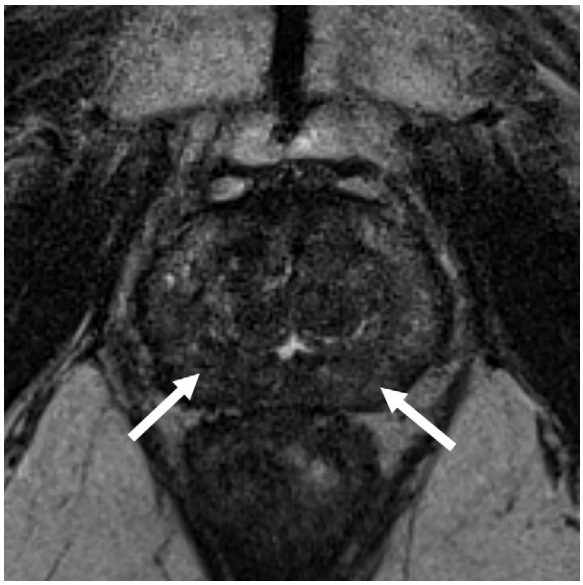

Figure 2. Normal posttreatment appearance in a 74-year-old man after external beam RT 5 years prior with a rising PSA level of 2 ng/mL from a nadir of 0.01 ng/mL. Axial T2-weighted MR image shows typical findings in the prostate gland after RT, with atrophy, diffuse T2-intermediate to hypointense signal (arrows), and loss of zonal anatomic distinction between the PZ and TZ.

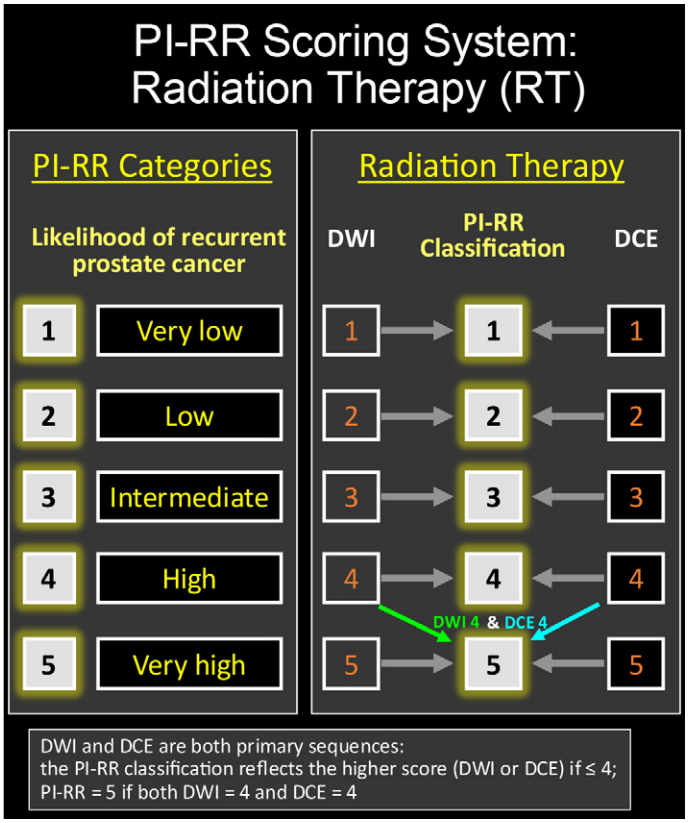

Figure 3. Flowchart for PI-RR scoring after RT. Note that DWI and DCE imaging are codominant sequences, with the higher of either score determining the ultimate PI-RR designation. If both DWI and DCE imaging are scored as 4, the final PI-RR score is 5.

signal intensity abnormality is assigned a score of 2 in PI-RR (Fig 5). The PI-RR 3 and 4 designations are similar to those in PI-RADS 2.1. Unlike PI-RADS 2.1, there is no size threshold nor requirement for extraprostatic extension to advance from a designation of 4 to 5 but rather correspondence of the abnormality to the site of the primary tumor. If at a different site (or the site of primary tumor is unknown), then a designation of 4 is given to a focal marked DWI and ADC signal abnormality.

Due to susceptibility artifact from brachytherapy seeds or fiducial markers for external beam radiation guidance degrading DWI in the post-RT prostate gland, DCE imaging is often the key sequence in assessing the post-RT gland (36). The pattern and timing of enhancement are important to assess, as diffuse or heterogeneous enhancement is assigned a DCE designation of 2, and late enhancement is assigned a designation of 3, even if focal or masslike (Fig 6). Early focal or masslike enhancement results in a characterization of 4 or 5, with foci at the site of primary tumor earning the designation of 5.

DWI and DCE imaging are considered codominant sequences for PI-RR scoring after RT, with the higher of either score resulting in the final PI-RR characterization. If both the DWI and DCE imaging scores are 4, then a final designation of PI-RR 5 is assigned based on the supposition that the combination of both DWI and DCE imaging abnormalities increases the likelihood of recurrent prostate cancer, even if not at the site of the primary tumor or if the site of primary tumor is either unknown or known to be spatially distinct from the finding of concern (20).

Radical Prostatectomy

The intent of RP is removal of the prostate gland and seminal vesicles, with or without pelvic lymph node dissection. Remnant seminal vesicles are present in up to 20% of patients who underwent RP and should not be mistaken for residual or recurrent tumor (37). There is a typical funneled appearance of the bladder neck and VUA after RP at coronal imaging (Fig 7) (38). The VUA and perianastomotic region is the most common site of local recurrence after RP. Other potential sites include the rectovesical space, seminal vesicles, pelvic floor abutting the levator ani muscles, and, less commonly, the penis (39,40). DCE is the key determinant of PI-RR scoring after RP, with recurrence resembling the primary tumor with early focal enhancement (Fig 8). Diffusion restriction may be present but is an ancillary feature in upgrading DCE scores of 2 or 3. The early enhancement of recurrent tumor should be distinguished from fibrous tissue, which typically exhibits late enhancement (36). If recurrence is detected at the VUA (the center of the clock), PI-RR recommends localization using a clock-face position.

After RP, the VUA is typically T2 hypointense (Fig 9) (38). Diffuse VUA thickening, thick-walled seminal vesicle remnants, or coarse scar tissue constitute a T2 score of 2, with symmetric focal or masslike thickening constituting a T2 score of 3. Asymmetric focal or masslike iso- or hyperintensity in these regions constitutes a T2 score of 4, upgraded to 5 if on the same side as the primary tumor. Abnormal T2 signal intensity is typically between that of muscle and fat (4). The morphology of post-RP recurrence varies from rounded lesions to plaquelike or curvilinear tissue (4). As with RT, RP scoring with PI-RR does not use the T2 score in final characterization.

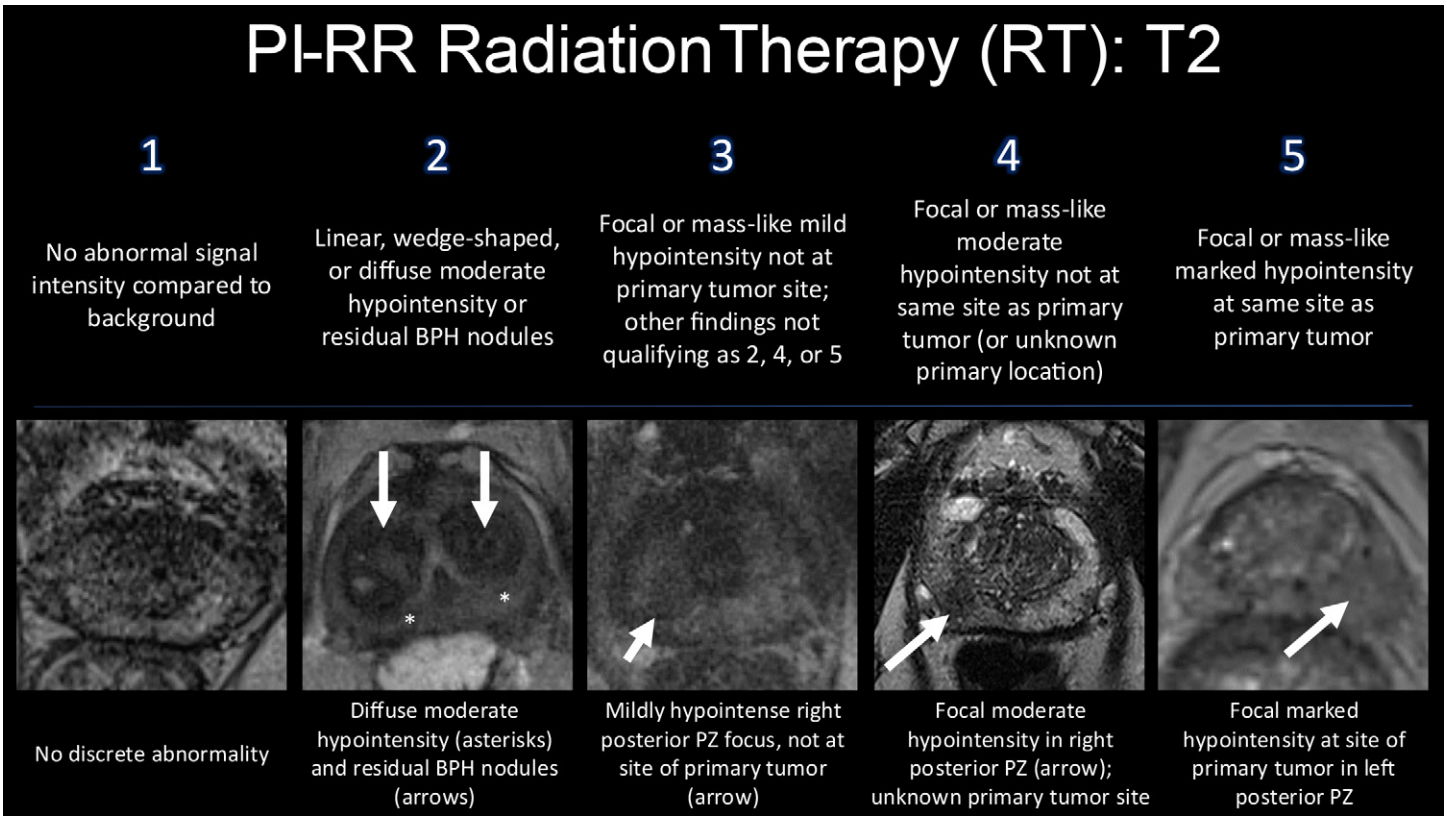

Figure 4. PI-RR T2 scoring for RT. Note that T2-weighted imaging *(T2)* does not factor into the final PI-RR designation but can be used for anatomic localization. *BPH* = benign prostatic hyperplasia.

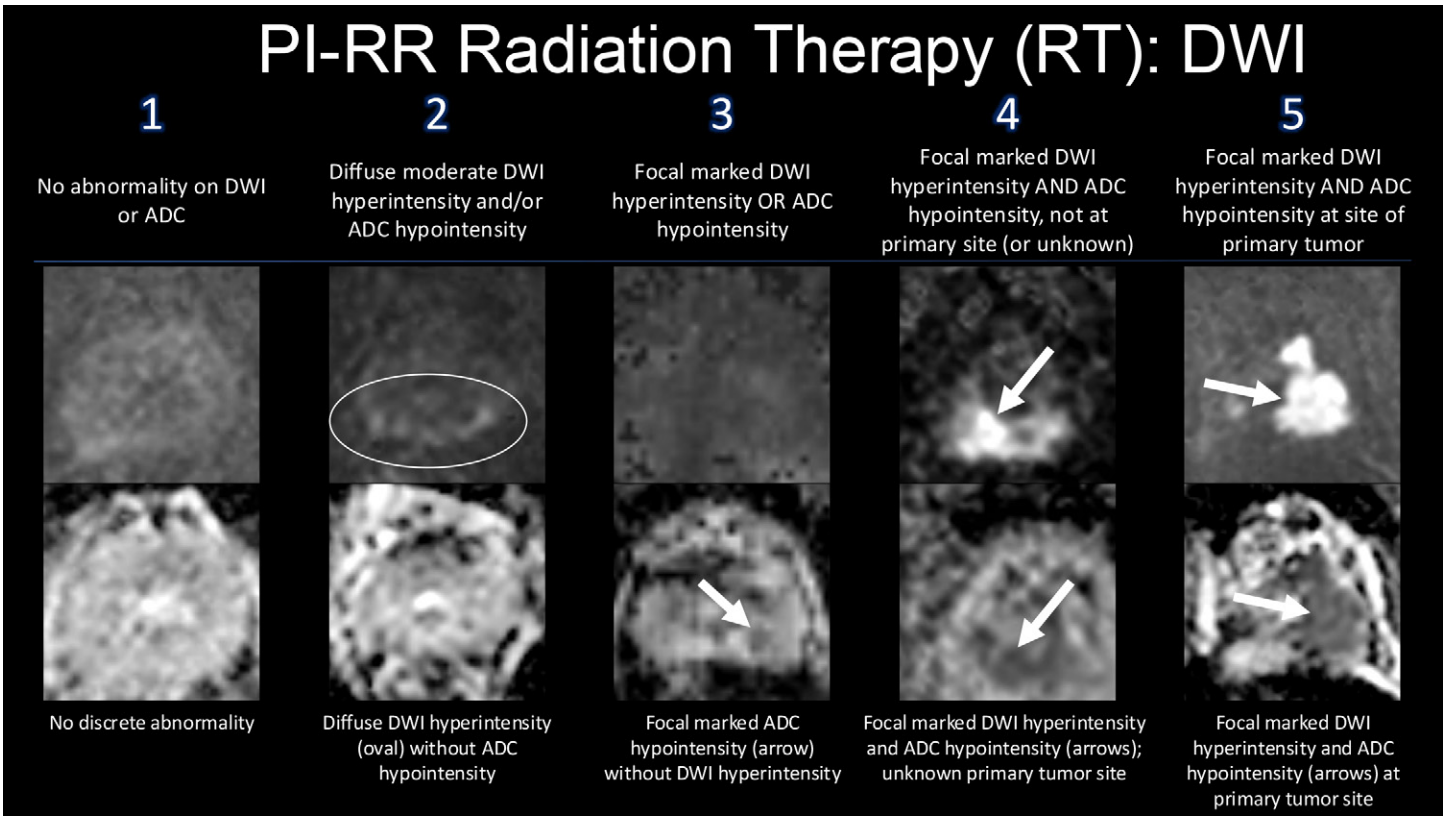

Figure 5. PI-RR DWI scoring for RT.

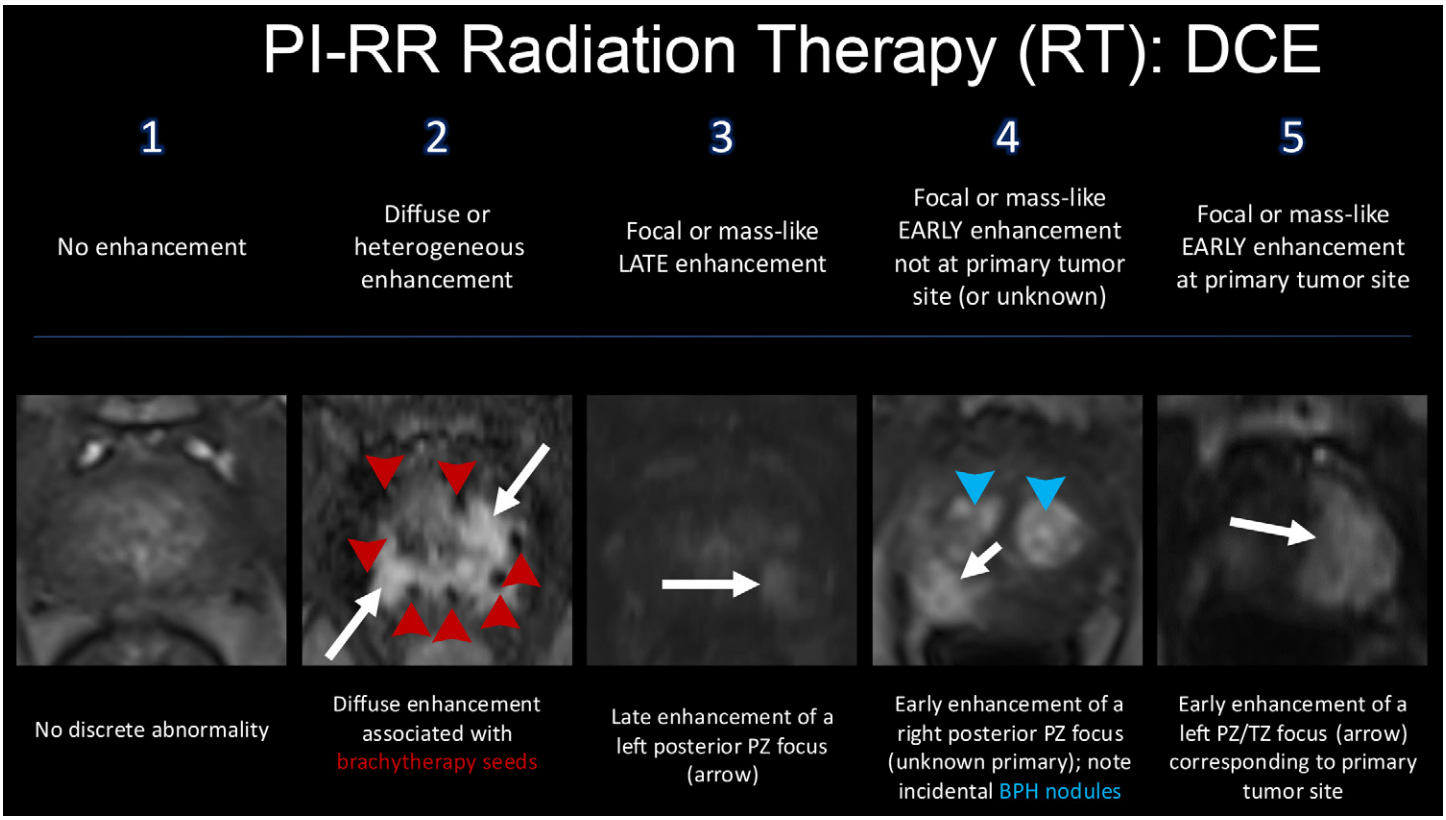

Figure 6. PI-RR DCE scoring for RT. *BPH* = benign prostatic hyperplasia.

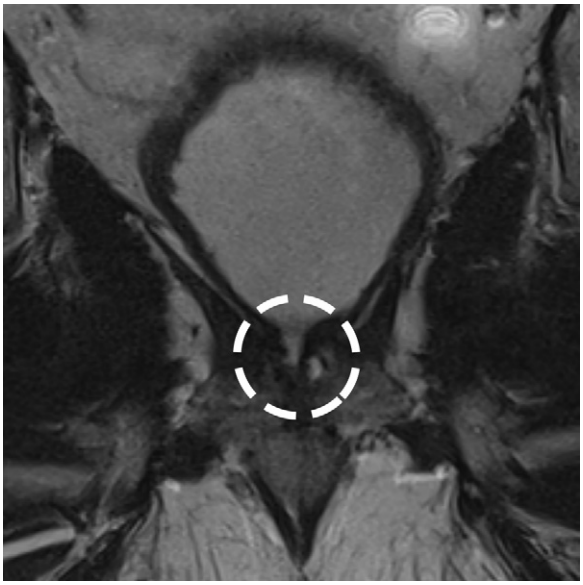

Figure 7. Normal postoperative appearance in a 73-year-old man after RP 10 years prior with a rising PSA level. Coronal T2-weighted MR image shows a normal appearance after RP. The VUA (dashed circle) is the most common site of recurrence. Subtle recurrence is less commonly identifiable at T2-weighted imaging than at DCE imaging.

DWI abnormalities after RP are assigned using a similar scoring rubric as that for RT, with focal marked DWI hyperintensity and ADC hypointensity conferring the greatest degree of suspicion (Fig 10). The exception is that distinction between the designation of 4 and 5 rests on laterality of the finding corresponding to the side of the primary tumor resulting in a score of 5, whereas contralateral abnormalities or an unknown primary site results in a score of 4. Susceptibility artifact from clips or other surgical material may limit the diagnostic utility of DWI after RP.

DCE imaging is the primary sequence for determining the PI-RR score after RP (Fig 11), offering high sensitivity even for small foci of disease, which exhibit focal or masslike early enhancement (13,14). The RP scoring system again mimics the corresponding DCE scoring rubric for RT, with the key distinction of the laterality of an early enhancing focus corresponding to the side of primary tumor distinguishing a score of 5 versus 4. Late enhancement and diffuse or heterogeneous enhancement are considered less suspicious, with scores of 3 and 2, respectively. Analysis of the VUA on multiplanar reformats of early DCE images can be helpful in detecting asymmetric early focal enhancement.

DCE imaging is the dominant sequence for RP scoring, solely determining the final PI-RR score when the DCE score is 1, 4, and 5. DCE scores of 2 and 3 can upgraded to 3 and 4, respectively, if a corresponding DWI abnormality with a score of 4 or more is present. This is analogous to the PI-RADS 2.1 TZ scoring upgrade system, where DWI serves as an adjunct parameter.

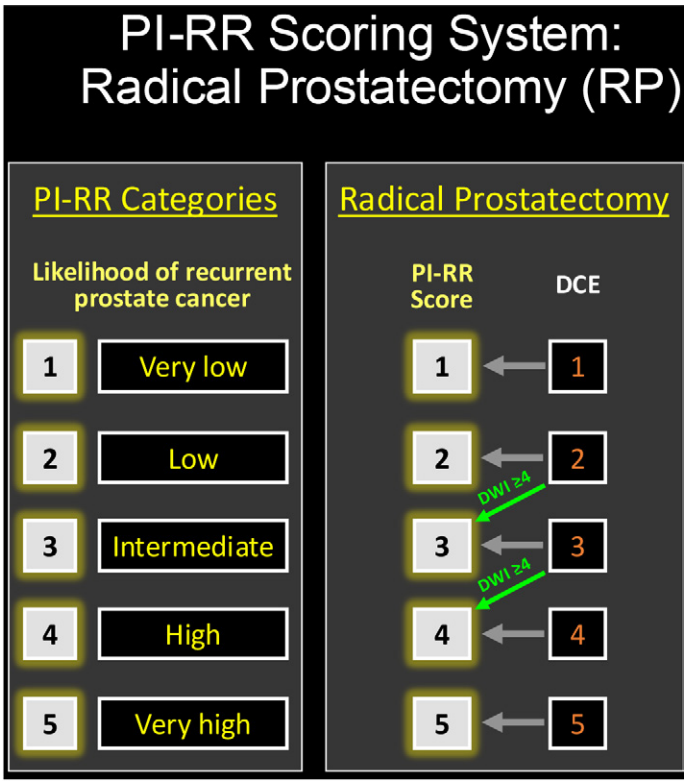

Figure 8. Flowchart for PI-RR scoring after RP. DCE is the sole determinant of the ultimate PI-RR scores, except with intermediate scores of 2 and 3, in which DWI scores of 4 or 5 will upgrade the PI-RR score by one point.

Case Examples

PI-RR Scoring after RT

Figure 12 shows an example of application of PI-RR in assessing for recurrent prostate cancer after external beam RT after BCR. In this case, a PI-RR score of 5 would be achieved even if the site of original tumor was not known on the basis of both a suspicious DWI and DCE imaging abnormality. PSMA PET/CT, although not currently integrated into PI-RR, provides value in directing attention to suspected sites of disease if performed before MRI (12). Figure 13 shows PI-RR scoring after a combination of external beam RT and high-dose-rate brachytherapy. As in many cases after RT, T2-weighted imaging is unhelpful as the gland is diffusely T2 hypointense, but the combination of DCE imaging and DWI leads to a categorization of PI-RR 5.

Figure 14 shows typical findings after low-dose-rate brachytherapy, with a diffusely hypointense appearance of the treated gland and loss of zonal anatomic distinction (41). DCE imaging proves to be the most valuable sequence, as the DWI abnormality in this case is less suspicious. This case also illustrates the importance of having either pretreatment imaging or pathology data from the primary tumor, as a score of 5 is otherwise not achievable in this case.

PI-RR Scoring after RP

The VUA is one of the most common sites of recurrence after RP and must be carefully scrutinized for asymmetries in enhancement. Figure 15 shows a case in which both DWI and DCE imaging are abnormal, but in the authors' experience (and as

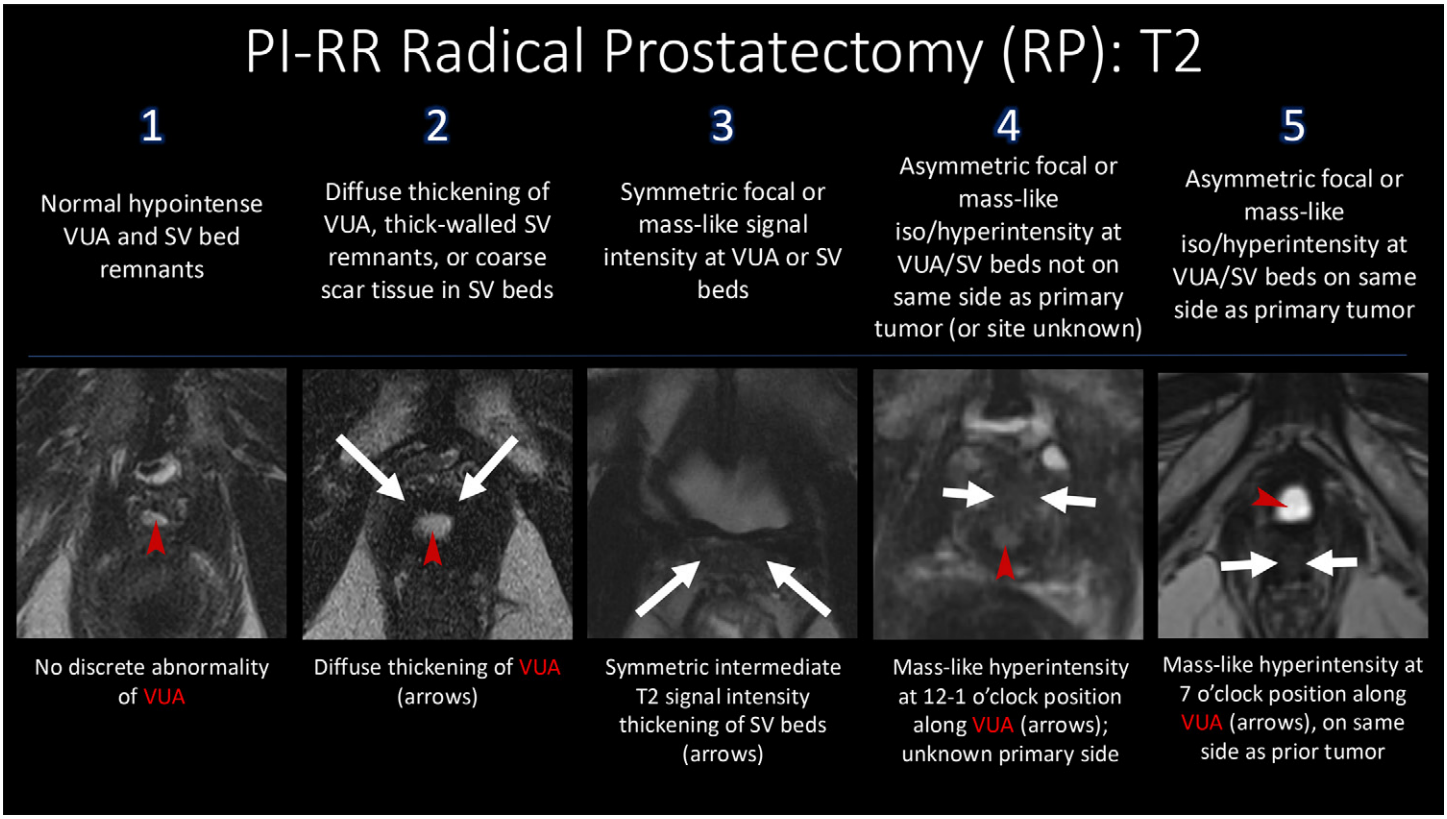

Figure 9. PI-RR T2-weighted imaging *(T2)* scoring for RP. As with RT, T2-weighted imaging does not factor into the final PI-RR designation after RP but can be used for anatomic localization. *SV* = seminal vesicle.

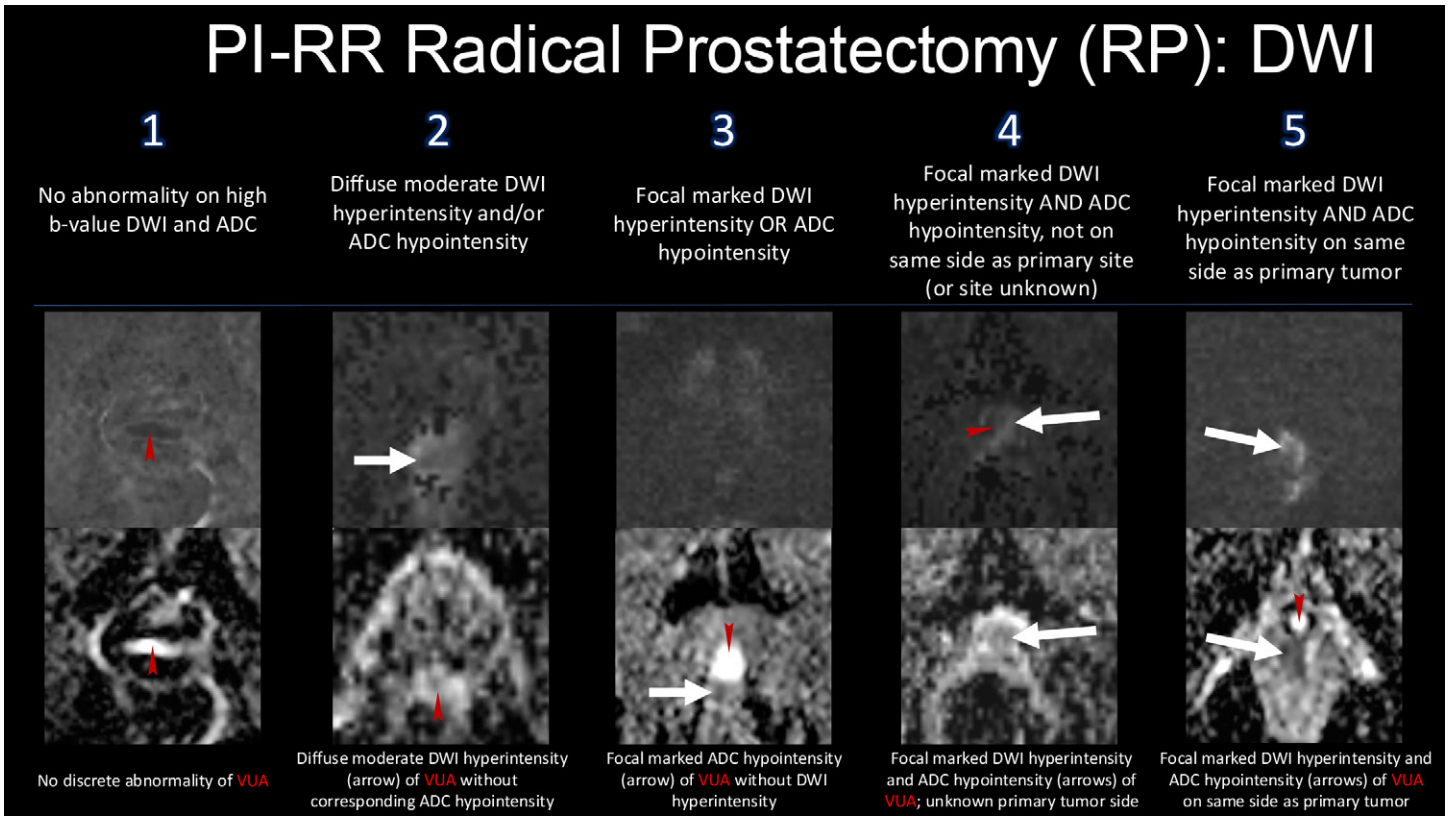

Figure 10. PI-RR DWI scoring for RP. A DWI score of 4 or 5 can upgrade low or intermediate suspicious DCE findings to a score of 2 or 3.

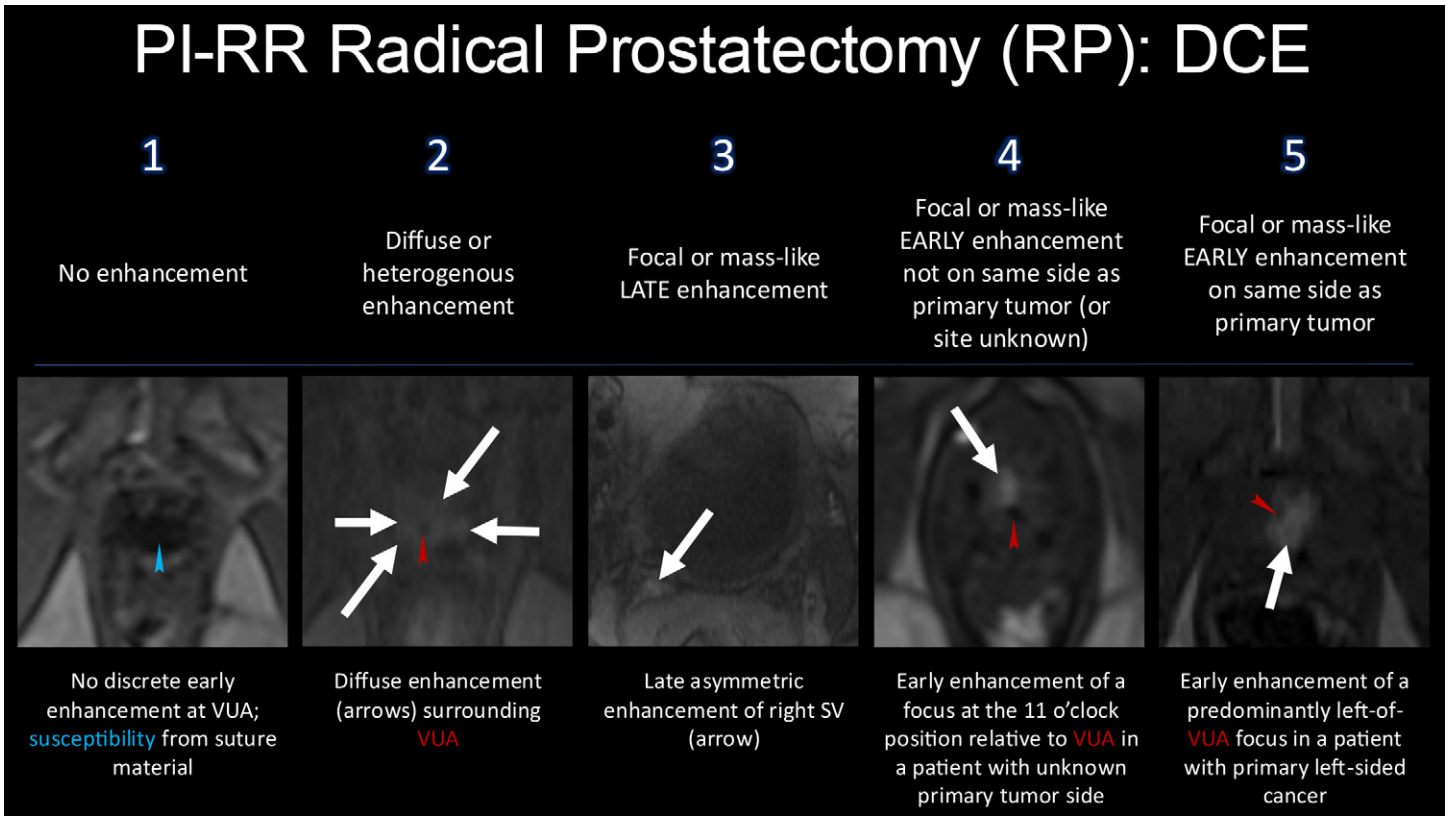

Figure 11. PI-RR DCE scoring for RP. *SV* = seminal vesicle.

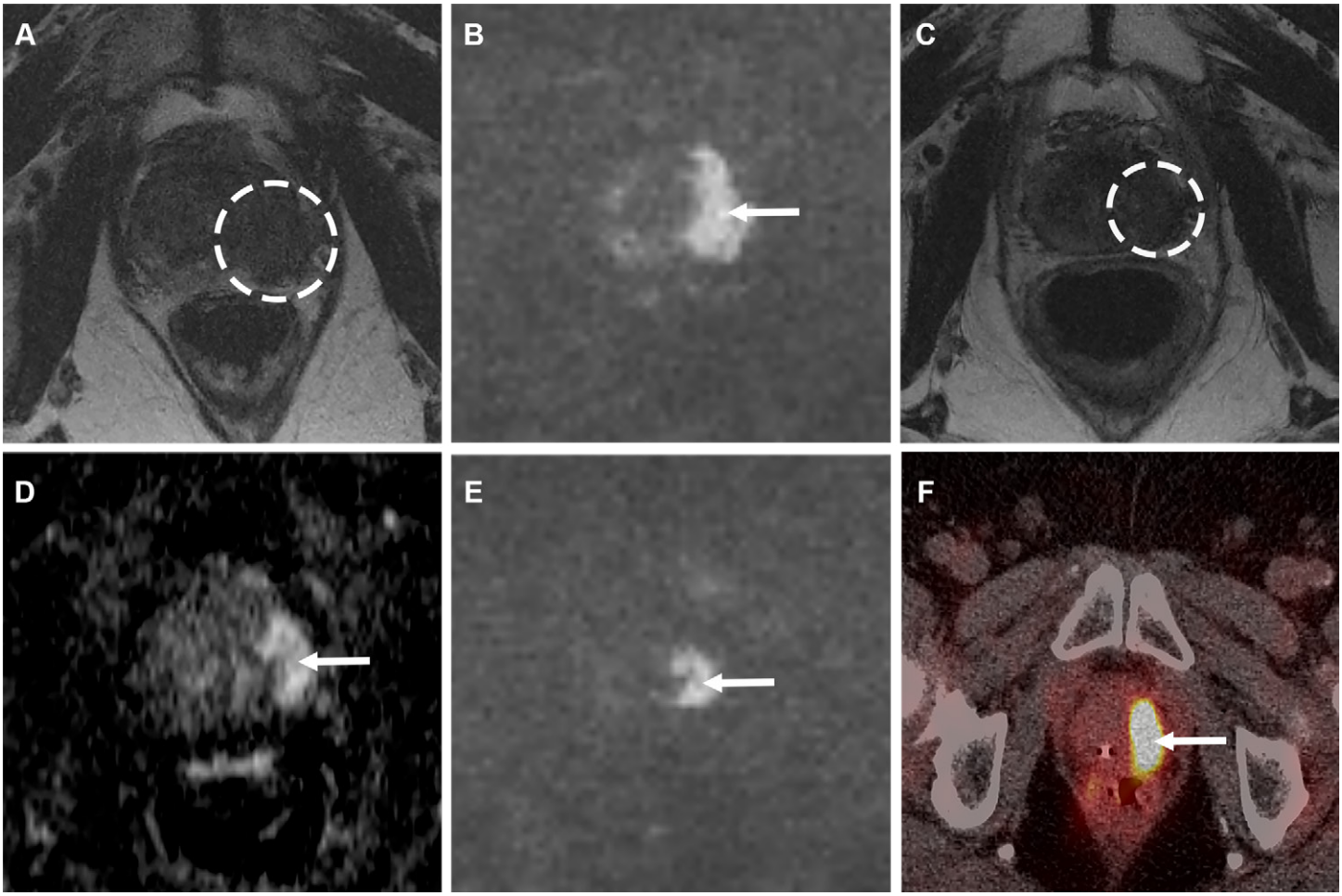

Figure 12. Prostate cancer recurrence after RT (PI-RR 5) in an 84-year-old man with prostate cancer (Gleason score 3 + 4) treated 3 years prior, with a rising PSA level from a nadir of 0.24 ng/mL to 2.68 ng/mL over a period of 2 years. **(A)** Axial T2-weighted MR image at diagnosis shows masslike rounded T2 hypointensity in the apex left lateral PZ (dashed circle). **(B)** Axial diffusion-weighted MR image at diagnosis shows corresponding marked hyperintensity of the original tumor (arrow). **(C)** Axial T2-weighted MR image at BCR shows focal hypointensity at the original tumor site (dashed circle) (T2 score of 5). **(D)** Axial DCE MR image at BCR shows corresponding focal masslike early enhancement at the original tumor site (arrow) (DCE score of 5). **(E)** Axial diffusion-weighted MR image at BCR shows focal hyperintensity at the original tumor site (arrow) (DWI score of 5). **(F)** Axial fused PSMA PET/CT image shows uptake at the original tumor site (arrow). The overall PI-RADS designation in this case is 5, achieved by either a DCE score of 5 or a DWI score of 5. The patient was placed on surveillance with a plan to treat with intermittent androgen deprivation therapy if PSA levels are greater than 10 ng/mL.

supported by the PI-RR scoring system), DCE imaging provides the highest value in detecting recurrence. Knowledge of the side of the original tumor allows an upgrade from a PI-RR score of 4 to 5 in this case.

The rectovesical space is another common site of recurrence after RP. Figure 16 shows a case in which there is extensive recurrence in the rectovesical space, extending into the bladder neck and across the mesorectal fascia to the anterior rectal wall. Seminal vesical remnants are uncommon sites of disease recurrence after RP but should be carefully assessed, as in Figure 17. MRI adds value when a potential abnormality at PSMA PET/CT is difficult to discern from activity in the adjacent bladder (12,42).

2/25/2026

Pitfalls and Limitations

Site and Laterality of Index Tumor

Unlike PI-RADS 2.1, in which differentiation between a category of high suspicion (score 4) and very high suspicion (score 5) is based on size and/or invasive behavior, PI-RR uses site or laterality of the primary tumor as the key determinant for post-RT and post-RP imaging, respectively. Pretreatment imaging is frequently unavailable, in the authors' experience, particularly for patients initially treated either at other centers or before the widespread adoption of prostate MRI. The assessment of findings that are predominantly midline after RP is not addressed, such as midline focal early enhancement along the VUA. The laterality of a positive surgical margin for midline tumors would logically serve as a surrogate to use as the "side" of the primary tumor but is not specifically addressed by PI-RR. The post-RT scoring rubric does offer the ability to upgrade to PI-RR 5 if both DWI and DCE scores of 4 are present. However, there is no ability to upgrade to a score of 5 if DCE imaging shows an obvious recurrence but DWI is degraded by magnetic susceptibility, when the index site of tumor is either unknown or different than the current finding.

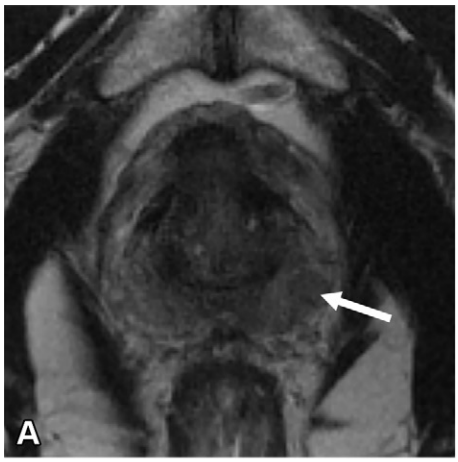

Figure 13. Recurrent prostate cancer after RT (PI-RR 5) in a 72-year-old man with left-sided prostate cancer (Gleason score 4 + 4) treated with external beam RT, high-dose-rate brachytherapy, and androgen deprivation therapy, with a PSA level subsequently rising from a nadir of less than 0.1 ng/mL to 13.3 ng/mL over a period of 16 months. **(A)** Axial T2-weighted MR image at diagnosis 4 years prior shows the index lesion in the left lateral base (arrow). **(B)** Axial T2-weighted MR image at BCR shows diffuse hypointensity (dashed circle) in the left base at the site of the original tumor (T2 score of 2). **(C)** Axial DCE MR image at BCR shows focal masslike early enhancement (arrow) at the original tumor site (DCE score of 5). **(D)** Axial diffusion-weighted MR image at BCR shows focal marked diffusion restriction (arrow) at the original tumor site (DWI score of 5). The overall PI-RR score is 5 based on either the DWI or DCE score of 5. The patient underwent additional high-dose-rate brachytherapy, treatment with triptorelin, and proton RT.

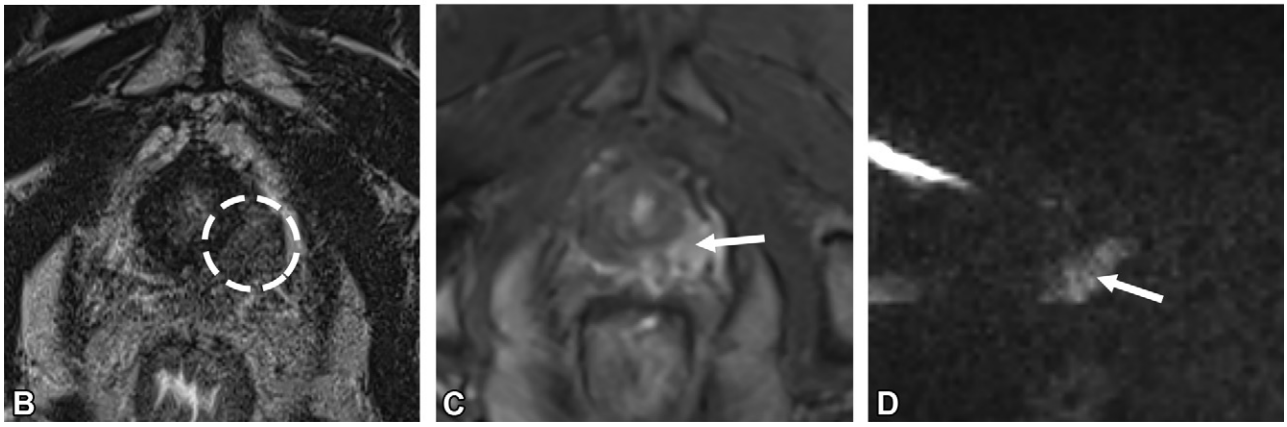

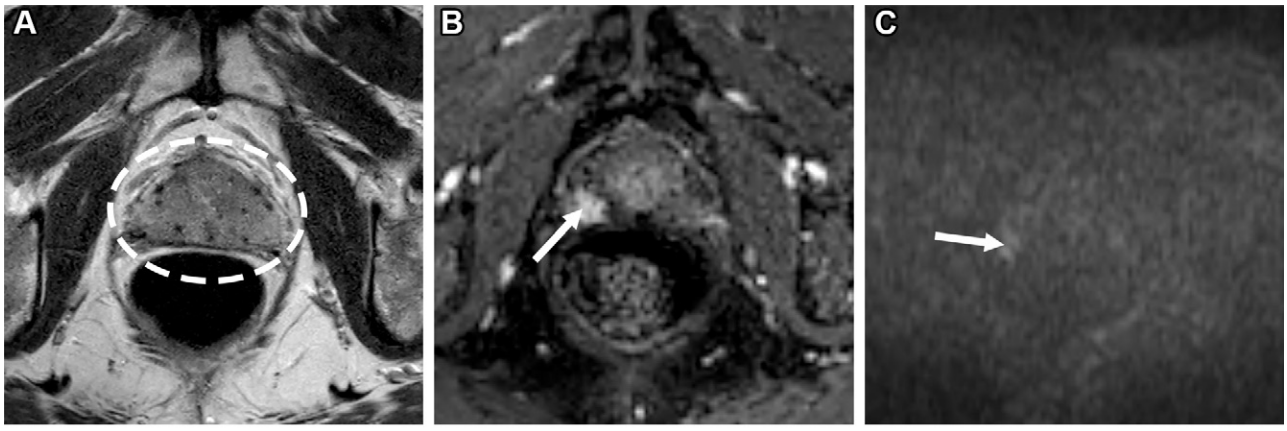

Figure 14. Recurrent prostate cancer in a 64-year-old man with prostate cancer (Gleason score 3 + 4; unknown original tumor site) treated with low-dose-rate brachytherapy and androgen deprivation therapy 8 years prior, now with an elevated PSA level of 3.3 ng/mL rising from a nadir of <0.1 ng/mL 5 years prior. **(A)** Axial T2-weighted MR image shows diffuse T2 hypointensity, atrophy, and loss of zonal anatomic distinction of the prostate gland (dashed oval) after brachytherapy (T2 score of 2). **(B)** Axial DCE MR image shows focal masslike early enhancement (arrow) (DCE score of 4). **(C)** Axial diffusion-weighted image shows faint hyperintensity (arrow) without corresponding ADC hypointensity (not shown) (DWI score of 3). **(D)** Axial fused PSMA PET/CT image shows marked focal tracer uptake, at the same location as the DCE abnormality, consistent with a site of recurrent prostate cancer (arrow). The overall PI-RR score is 4 (the higher of the DCE and DWI scores), and the patient underwent salvage focal cryoablation.

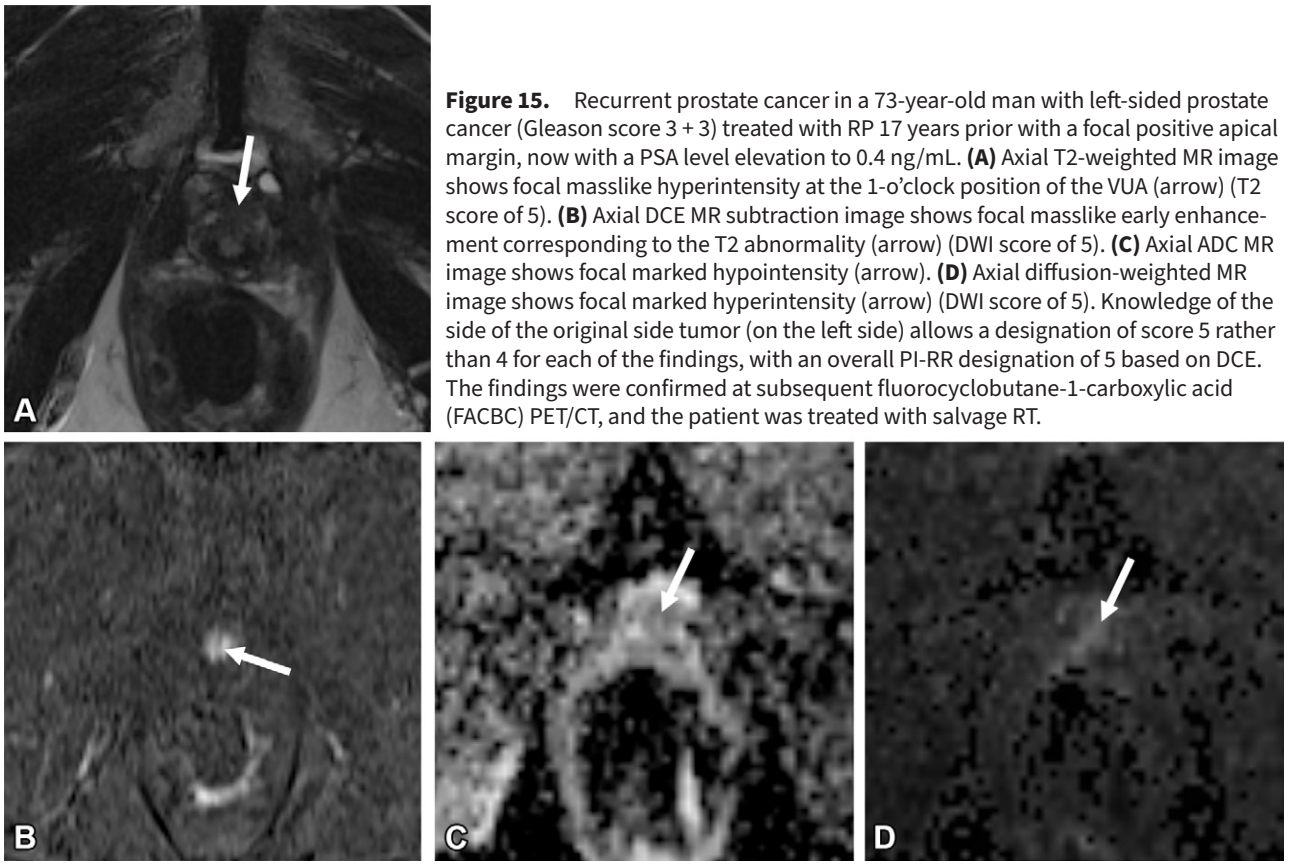

Figure 15. Recurrent prostate cancer in a 73-year-old man with left-sided prostate cancer (Gleason score 3 + 3) treated with RP 17 years prior with a focal positive apical margin, now with a PSA level elevation to 0.4 ng/mL. **(A)** Axial T2-weighted MR image shows focal masslike hyperintensity at the 1-o'clock position of the VUA (arrow) (T2 score of 5). **(B)** Axial DCE MR subtraction image shows focal masslike early enhancement corresponding to the T2 abnormality (arrow) (DWI score of 5). **(C)** Axial ADC MR image shows focal marked hypointensity (arrow). **(D)** Axial diffusion-weighted MR image shows focal marked hyperintensity (arrow) (DWI score of 5). Knowledge of the side of the original side tumor (on the left side) allows a designation of score 5 rather than 4 for each of the findings, with an overall PI-RR designation of 5 based on DCE. The findings were confirmed at subsequent fluorocyclobutane-1-carboxylic acid (FACBC) PET/CT, and the patient was treated with salvage RT.

Figure 16. Recurrent prostate cancer in a 74-year-old man with prostate cancer (Gleason score 3 + 4) treated with RP 27 years prior, with subsequent RT and intermittent androgen deprivation therapy, now with a PSA level elevation of 22.8 ng/mL. **(A)** Axial T2-weighted MR image shows a focal T2-hypointense mass adjacent to the bladder neck involving both ureterovesical junctions (arrows) (T2 score of 5). **(B)** Axial DCE MR image shows corresponding focal masslike early enhancement of the lesion (arrows) (DCE score of 5). **(C)** Axial ADC MR image shows corresponding marked hypointensity of the mass (arrows). DWI exhibited corresponding marked hyperintensity (not shown), giving a DWI score of 5. **(D)** Axial T2-weighted MR image at a more inferior level shows abutting of the anterior rectum (dashed oval) by the mass (arrow). The overall PI-RR score is 5 based on DCE. Due to the presence of metastatic lymphadenopathy and bone metastases, the patient was treated with systemic chemotherapy and subsequently with PSMA-directed radioligand therapy.

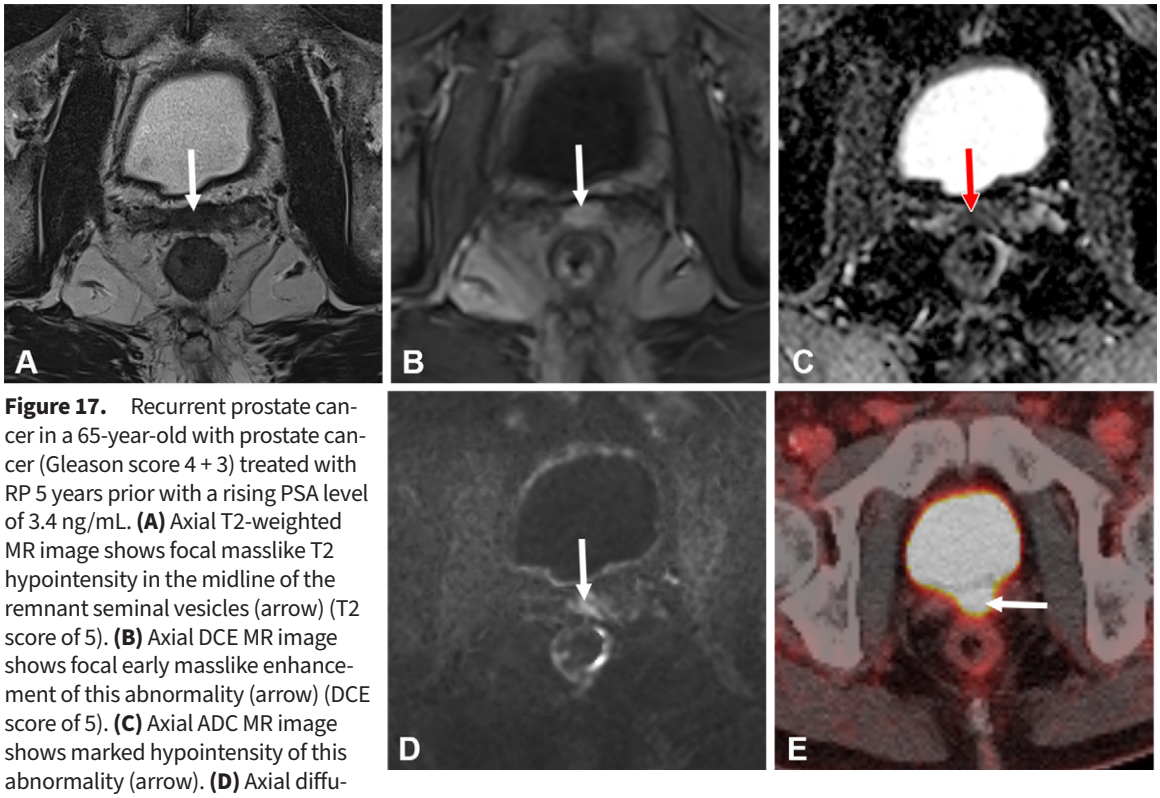

Figure 17. Recurrent prostate cancer in a 65-year-old with prostate cancer (Gleason score 4 + 3) treated with RP 5 years prior with a rising PSA level of 3.4 ng/mL. **(A)** Axial T2-weighted MR image shows focal masslike T2 hypointensity in the midline of the remnant seminal vesicles (arrow) (T2 score of 5). **(B)** Axial DCE MR image shows focal early masslike enhancement of this abnormality (arrow) (DCE score of 5). **(C)** Axial ADC MR image shows marked hypointensity of this abnormality (arrow). **(D)** Axial diffusion-weighted MR image shows marked hyperintensity of this abnormality (arrow) (DWI score of 5). **(E)** Axial PSMA PET/CT image shows increased activity (arrow), although it is difficult to discern from bladder activity more anteriorly. The overall PI-RR score is 5, and the patient underwent salvage radiation, with a subsequently undetectable PSA level.

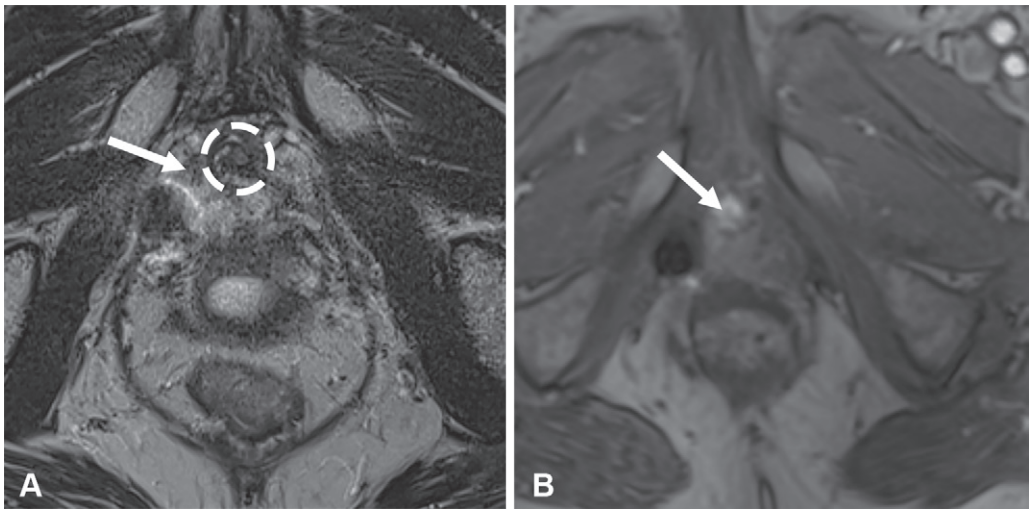

Figure 18. Residual prostate tissue in a 72-year-old man with prostate cancer (Gleason score 4 + 3) treated with prostatectomy 19 years prior, with a gradual increase in PSA level to 1.2 ng/mL. **(A)** Axial T2-weighted MR image shows vague hypointensity to the right (arrow) of the VUA (dashed circle). **(B)** Axial DCE MR image shows focal late masslike enhancement of this lesion (DCE score of 3). DWI was unrevealing (not shown). Biopsy revealed benign residual prostatic tissue without local recurrence. The patient was subsequently found to have systemic recurrence at PSMA PET/CT in the right upper lobe (not shown), managed with wedge resection.

Residual Prostate or Seminal Vesicle Tissue

The prevalence of detectable remnant prostate tissue at MRI after prostatectomy is approximately 1%–3% (Fig 18) (43). This benign remnant tissue exhibits MRI characteristics that differ from the expected appearance of recurrent prostate cancer, such as higher T2 signal intensity and absent diffusion restriction. Seminal vesicle remnants are more common, seen in up to 20% of cases after RP, and should be recognized to avoid misinterpretation as local recurrence (Fig 19).

Normal Postoperative Structures

Several normal structures in the postoperative pelvis after RP may parallel the appearance of recurrent prostate cancer (44). The cuff of the vas deferens after RP and seminal vesiculectomy may mimic local recurrence at T2-weighted imaging when mildly thickened or enhancing but should not enhance in a rapid fashion or exhibit marked diffusion restriction as would recurrent prostate cancer. The membranous urethra at the VUA may also hyperenhance and is challenging to distinguish from recurrent tumor, although circumferential

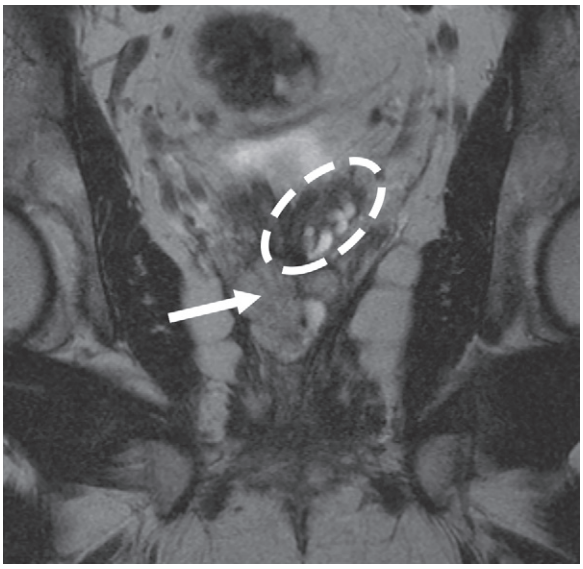

Figure 19. Residual seminal vesicle and prostate tissue in a 63-year-old man with prostate cancer (Gleason score 4 + 5) treated with RP 14 months prior with an elevated PSA level of 1.7 ng/mL. Coronal T2-weighted MR image shows both residual right prostate PZ (arrow) and residual left seminal vesicle tissue (dashed oval). Diffuse enhancement was noted at DCE imaging (not shown; DCE score of 2), resulting in a PI-RR score of 2.

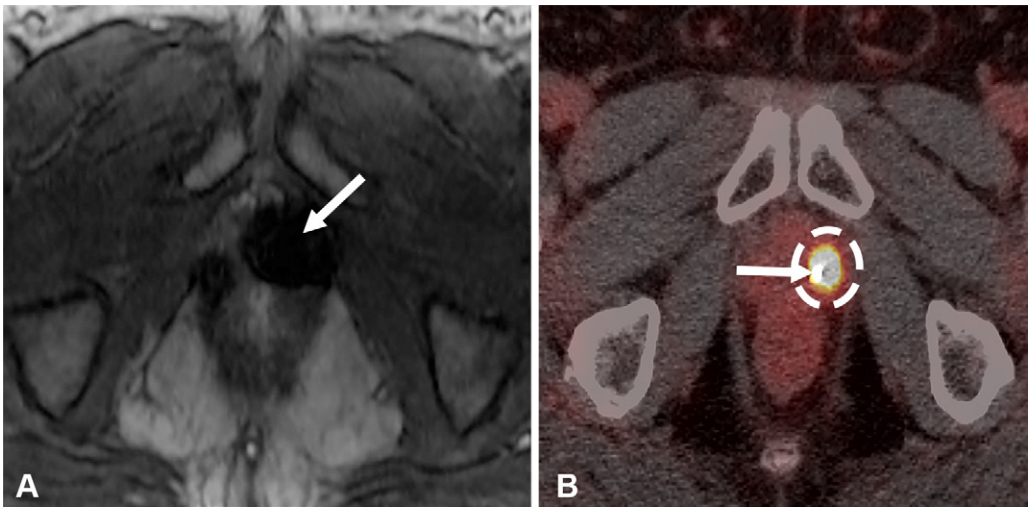

Figure 20. Susceptibility artifact obscuring recurrence in a 69-year-old man with prostate cancer (Gleason score 3 + 3) treated with RT 13 years prior with an elevated PSA level of 3.4 ng/mL. **(A)** Axial DCE MR image shows susceptibility artifact (arrow) from a fiducial marker, obscuring a portion of the prostate gland. **(B)** Axial fused PSMA PET/CT image shows a focus of uptake (oval) in the obscured region representing recurrent tumor adjacent to the fiducial marker (arrow). The patient was treated with high-dose-rate brachytherapy.

enhancement may favor benignity. The mount of thickened bladder neck at the VUA may also simulate the appearance of recurrent tumor, although again focality rather than diffuse thickening may favor malignancy.

Magnetic Susceptibility Artifact

Surgical clips, brachytherapy seeds, and fiducial markers frequently create magnetic susceptibility artifacts that may limit evaluation, particularly with sensitive sequences such as DWI and to a lesser extent DCE imaging (Fig 20) (45). The metal composition influences the degree of artifact, with relatively low magnetic susceptibility from substances such as titanium (brachytherapy) and gold or platinum (fiducial markers) compared with other metals used in implants, such as cobalt-chromium alloys or stainless steel (46,47). High-dose-rate brachytherapy does not result in susceptibility as the flexible seeds that are inserted to deliver radiation over a period of a few minutes are not left in place, unlike the permanent seeds of low-dose rate brachytherapy (48). Brachytherapy seeds commonly migrate inferiorly after the radiation-induced atrophy of the prostate gland, leading to potential degradation of dose coverage and risk of local treatment failure. Mitigation of susceptibility artifact can be attempted with high-bandwidth and view-angle-tilting techniques for turbo spin-echo T2-weighted imaging and using multishot readout segmented echo-planar imaging techniques for DWI. As PI-RR does not integrate T2-weighted scoring into the final designation, diagnostic T2-weighted imaging might highlight the potential location of recurrence better than DCE imaging or DWI but will not contribute to the final score.

Future Developments

Focal Therapy

PI-RR is intended for use in assessing recurrence after whole-gland therapies such as RT and RP but does not address imaging after focal therapy. Focal therapies are an alternative for treating low-volume intermediate-risk prostate cancer with the promise of minimal functional impairment (49). Current available technologies include cryoablation, high-intensity focused US, laser ablation, irreversible electroporation, and vascular-targeted photodynamic therapy, with additional new technologies on the horizon (50). Partial ablations can be targeted, cover a defined region such as a quadrant or hemigland, or even be subtotal in coverage. Although PI-RR does not address imaging after focal therapy, other systems have been proposed, such as the Prostate Imaging after Focal Ablation (PI-FAB) scoring system, which differs from other prostate imaging scoring systems in using a 1–3 rather than 1–5 scale to indicate the degree of suspicion (51–53), and the Transatlantic Recommendations for Prostate Gland Evaluation with Magnetic Resonance Imaging After Focal Therapy (TARGET) consensus (54). Conceivably, future iterations of PI-RR and focal therapy imaging systems could be subsumed under PI-RADS itself to have a unified approach under a larger umbrella, such as with the Liver Imaging and Reporting Data System (LI-RADS) and its various offshoots.

Androgen Deprivation Therapy

Androgen deprivation therapy is frequently used as neoadjuvant therapy before RP or in conjunction with RT (55). PI-RR does not currently specifically address the imaging of patients treated with androgen deprivation therapy or patients treated with multimodality therapy. Chen et al (56) assessed the performance of PI-RR for detection of residual prostate cancer after androgen deprivation therapy in a cohort of 119 patients treated with neoadjuvant androgen deprivation therapy before RP and found sensitivity of 74.2%–83.7%, specificity of 86.4%–92.7%, a positive predictive value of 51.3%–64.3%, and a negative predictive value of 95.4%–96.9%, respectively, using a PI-RR score of 3 or greater as a cutoff and the RT scoring rubric (56). Future iterations of PI-RR could potentially specifically address imaging patients treated with androgen deprivation therapy alone.

PSMA PET

Since their approval by the U.S. Food and Drug Administration several years ago, PET tracers targeting the PSMA, a transmembrane protein that is commonly overexpressed by adenocarcinomas of prostate origin, have revolutionized prostate cancer imaging (57,58). In general, prostate MRI and PSMA PET/CT play complementary roles in the BCR setting, with the former providing precise anatomic localization of recurrent disease in the prostate gland or prostatectomy bed and the latter providing high detection rate for sites of nodal and distant metastatic disease (12,59,60). The combined review of prostate MRI and PSMA PET/CT examinations may facilitate the identification of disease sites that might go unrecognized when either examination is interpreted independently, and it is particularly helpful in distinguishing recurrence from urine activity (Fig 21) (42). Furthermore, abnormalities at prostate MRI that are deemed indeterminate (ie, PI-RR 3) should be viewed with greater suspicion if accompanied by focal abnormal PSMA expression.

There is a clinical need for long-term outcome prediction models utilizing MRI and PSMA PET. A study showed that patients with positive MRI for local recurrence without documented distant metastasis had better systemic progression-free survival rates but worse disease-specific survival than those with negative MRI (61). In the same study, larger lesion size significantly increased the risk of death from prostate cancer. The uncoupling of progression-free survival and disease-specific survival may be explained by the locally recurrent tumor burden, which may be better assessed with MRI than PSMA PET. Not only the presence or absence of locally recurrent tumor but also tumor volume in the prostatectomy bed may be an important prognostic consideration. A combination of MRI and PSMA PET may further improve the prediction of long-term clinical outcomes in patients with BCR by stratifying them into three categories: *(a)* local recurrence without metastasis, *(b)* metastasis without local recurrence, or *(c)* a combination of local recurrence and metastasis. As such, PSMA PET/MRI may be the ideal imaging study for patients with prostate cancer undergoing workup for BCR (62). In light of this synergy, future iterations of the PI-RR algorithm might achieve even higher diagnostic accuracy by incorporating PSMA PET findings when available.

Conclusion

PI-RR constructs a framework for systematic evaluation of the treated prostate after RP or RT using the familiar 1–5 Likert scoring scale. Having access to either the pretreatment imaging studies and/or knowledge of the site of the primary tumor informs both interpretation and scoring. PI-RR provides complementary information regarding local recurrence to the locoregional or distant staging data from PSMA PET/CT. Future iterations of PI-RR may address focal therapies and how to integrate functional modalities (eg, PSMA PET) for comprehensive evaluation of recurrent prostate cancer.

Author affiliations.—From the Mallinckrodt Institute of Radiology, Washington University School of Medicine, 510 S Kingshighway Blvd, Campus Box 8131, St Louis, MO 63110. Presented as an education exhibit at the 2023 RSNA Annual Meeting. Received April 30, 2024; revision requested June 4 and received June 7; accepted August 8. **Address correspondence to** A.S.S. (email: *anup.shetty@wustl.edu*).

Disclosures of conflicts of interest.—**D.H.B.** Consulting fees from Merck (ended in March 2024). All other authors, the editor, and the reviewers have disclosed no relevant relationships.

References

1. Siegel RL, Giaquinto AN, Jemal A. Cancer statistics, 2024. CA Cancer J Clin 2024;74(1):12–49 [Published correction appears in CA Cancer J Clin 2024;74(2):203.].
2. Hamdy FC, Donovan JL, Lane JA, et al. 10-Year Outcomes after Monitoring, Surgery, or Radiotherapy for Localized Prostate Cancer. N Engl J Med 2016;375(15):1415–1424.
3. Van den Broeck T, van den Bergh RCN, Briers E, et al. Biochemical Recurrence in Prostate Cancer: The European Association of Urology Prostate Cancer Guidelines Panel Recommendations. Eur Urol Focus 2020;6(2):231–234.

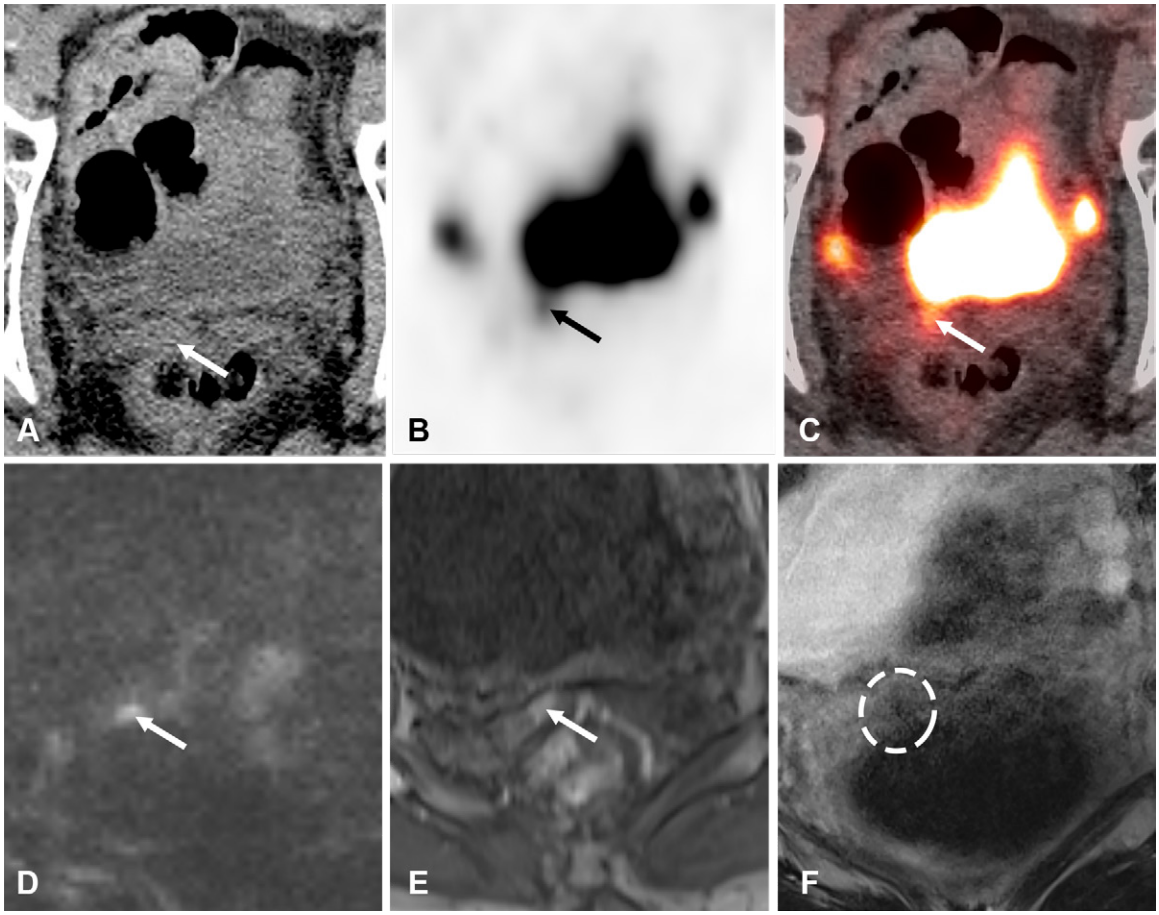

Figure 21. Recurrent prostate cancer in a 68-year-old man with prostate cancer (Gleason score 4 + 3) of the right PZ at the base treated with RT 3 years prior with a rising PSA level of 1.6 ng/mL from a nadir of 0.1 ng/mL 2 years prior. Prostate MRI findings were initially interpreted as negative. **(A–C)** Axial CT **(A)**, PET **(B)**, and fused PET/CT **(C)** images from subsequent PSMA PET/CT show an indeterminate focus of activity (arrow) localizing to the right seminal vesicle without an anatomic correlate at CT, representing recurrent disease versus artifact from the adjacent urinary bladder. In light of the PET findings, the prostate MRI study was reviewed again. **(D–F)** Axial diffusion-weighted **(D)**, DCE **(E)**, and T2-weighted **(F)** MR images show a focus of early hyperenhancement and marked diffusion restriction (arrow in **D** and **E**) corresponding to the PET abnormality, consistent with disease recurrence (PI-RR 5). There was no correlate on the T2-weighted image due to motion artifacts (dashed circle in **F**), highlighting the need for careful MRI review even if some sequences are degraded.

4. Panebianco V, Villeirs G, Weinreb JC, et al. Prostate Magnetic Resonance Imaging for Local Recurrence Reporting (PI-RR): International Consensus-based Guidelines on Multiparametric Magnetic Resonance Imaging for Prostate Cancer Recurrence after Radiation Therapy and Radical Prostatectomy. Eur Urol Oncol 2021;4(6):868–876.
5. Marcus DM, Canter DJ, Jani AB, et al. Salvage therapy for locally recurrent prostate cancer after radiation. Can J Urol 2012;19(6):6534–6541.
6. Morgan TM, Boorjian SA, Buyyounouski MK, et al. Salvage Therapy for Prostate Cancer: AUA/ASTRO/SUO Guideline Part I—Introduction and Treatment Decision-Making at the Time of Suspected Biochemical Recurrence after Radical Prostatectomy. J Urol 2024;211(4):509–517.
7. Silverman JM, Krebs TL. MR imaging evaluation with a transrectal surface coil of local recurrence of prostatic cancer in men who have undergone radical prostatectomy. AJR Am J Roentgenol 1997;168(2):379–385.
8. Cornford P, van den Bergh RCN, Briers E, et al. EAU-EANM-ESTRO-ESUR-SIOG Guidelines on Prostate Cancer. Part II: 2020 Update—Treatment of Relapsing and Metastatic Prostate Cancer. Eur Urol 2021;79(2):263–282.
9. Dotan ZA, Bianco FJ Jr, Rabbani F, et al. Pattern of prostate-specific antigen (PSA) failure dictates the probability of a positive bone scan in patients with an increasing PSA after radical prostatectomy. J Clin Oncol 2005;23(9):1962–1968.
10. Park KJ, Choi SH, Kim M-H, Kim JK, Jeong IG. Performance of Prostate Imaging Reporting and Data System Version 2.1 for Diagnosis of Prostate Cancer: A Systematic Review and Meta-Analysis. J Magn Reson Imaging 2021;54(1):103–112.
11. American College of Radiology. PI-RADS: Prostate Imaging—Reporting and Data System: Version 2.1. https://www.acr.org/-/media/ACR/Files/RADS/Pi-RADS/PIRADS-v2-1.pdf. Published 2019. Accessed April 2, 2024.
12. Awiwi MO, Gjoni M, Vikram R, et al. MRI and PSMA PET/CT of Biochemical Recurrence of Prostate Cancer. RadioGraphics 2023;43(12):e230112.
13. Park MY, Park KJ, Kim M-H, Kim JK. Focal nodular enhancement on DCE MRI of the prostatectomy bed: radiologic-pathologic correlations and prognostic value. Eur Radiol 2023;33(4):2985–2994.
14. Kitajima K, Hartman RP, Froemming AT, Hagen CE, Takahashi N, Kawashima A. Detection of Local Recurrence of Prostate Cancer After Radical Prostatectomy Using Endorectal Coil MRI at 3 T: Addition of DWI and Dynamic Contrast Enhancement to T2-Weighted MRI. AJR Am J Roentgenol 2015;205(4):807–816.
15. Kwon T, Kim JK, Lee C, et al. Discrimination of local recurrence after radical prostatectomy: value of diffusion-weighted magnetic resonance imaging. Prostate Int 2018;6(1):12–17.
16. De Visschere PJL, Standaert C, Fütterer JJ, et al. A Systematic Review on the Role of Imaging in Early Recurrent Prostate Cancer. Eur Urol Oncol 2019;2(1):47–76.
17. National Comprehensive Cancer Network. NCCN Prostate Cancer Clinical Practice Guidelines in Oncology. https://www.nccn.org/guidelines/guidelines-detail?category=1&id=1459. Published 2024. Accessed April 2, 2024.
18. Maurer T, Eiber M, Fanti S, Budäus L, Panebianco V. Imaging for Prostate Cancer Recurrence. Eur Urol Focus 2016;2(2):139–150.

19. Sandgren K, Westerlinck P, Jonsson JH, et al. Imaging for the Detection of Locoregional Recurrences in Biochemical Progression After Radical Prostatectomy: A Systematic Review. Eur Urol Focus 2019;5(4):550–560.
20. Pecoraro M, Turkbey B, Purysko AS, et al. Diagnostic Accuracy and Observer Agreement of the MRI Prostate Imaging for Recurrence Reporting Assessment Score. Radiology 2022;304(2):342–350.
21. Bergaglio C, Giasotto V, Marcenaro M, et al. The Role of mpMRI in the Assessment of Prostate Cancer Recurrence Using the PI-RR System: Diagnostic Accuracy and Interobserver Agreement in Readers with Different Expertise. Diagnostics (Basel) 2023;13(3):387.
22. Ciccarese F, Corcioni B, Bianchi L, et al. Clinical Application of the New Prostate Imaging for Recurrence Reporting (PI-RR) Score Proposed to Evaluate the Local Recurrence of Prostate Cancer after Radical Prostatectomy. Cancers (Basel) 2022;14(19):4725.
23. Franco PN, Frade-Santos S, García-Baizán A, et al. An MRI assessment of prostate cancer local recurrence using the PI-RR system: diagnostic accuracy, inter-observer reliability among readers with variable experience, and correlation with PSA values. Eur Radiol 2024;34(3):1790–1803.
24. Akkaya H, Topaloğlu AC, İzgi N, Soker G, Karaca F, Gülek B. Investigation of the Interobserver Variability of the Prostate Imaging for Recurrence Reporting (PI-RR) Score in Evaluating Local Recurrence in Prostate Cancer After Radiotherapy: Are Tumor Size and Prostate-specific Antigen Important? Van Med J 2023;30(2):200–208.
25. Kim M, Hwang SI, Ahn H, et al. Diagnostic yield of multiparametric MRI for local recurrence at biochemical recurrence after radical prostatectomy. Prostate Int 2022;10(3):135–141.
26. Woernle A, Englman C, Dickinson L, et al. Picture Perfect: The Status of Image Quality in Prostate MRI. J Magn Reson Imaging 2024;59(6):1930–1952.
27. Belue MJ, Yilmaz EC, Daryanani A, Turkbey B. Current Status of Biparametric MRI in Prostate Cancer Diagnosis: Literature Analysis. Life (Basel) 2022;12(6):804.
28. Shetty AS, Nigogosyan Z, Stephen V, et al. Body MRI Pulse Sequences: Atlas and User Guide. RadioGraphics 2024;44(1):e230085.
29. Salari R, Ballard DH, Hoegger MJ, Young D, Shetty AS. Fat-only Dixon: how to use it in body MRI. Abdom Radiol (NY) 2022;47(7):2527–2544.
30. Yu J-S, Chung J-J, Hong SW, Chung BH, Kim JH, Kim KW. Prostate cancer: added value of subtraction dynamic imaging in 3T magnetic resonance imaging with a phased-array body coil. Yonsei Med J 2008;49(5):765–774.
31. Verma S, Turkbey B, Muradyan N, et al. Overview of dynamic contrast-enhanced MRI in prostate cancer diagnosis and management. AJR Am J Roentgenol 2012;198(6):1277–1288.
32. Arrayeh E, Westphalen AC, Kurhanewicz J, et al. Does local recurrence of prostate cancer after radiation therapy occur at the site of primary tumor? Results of a longitudinal MRI and MRSI study. Int J Radiat Oncol Biol Phys 2012;82(5):e787–e793.
33. Wu X, Reinikainen P, Kapanen M, Vierikko T, Ryymin P, Kellokumpu-Lehtinen P-L. Monitoring radiotherapy induced tissue changes in localized prostate cancer by multi-parametric magnetic resonance imaging (MP-MRI). Diagn Interv Imaging 2019;100(11):699–708.
34. Pecoraro M, Dehghanpour A, Das JP, Woo S, Panebianco V. Evaluation of Prostate Cancer Recurrence with MR Imaging and Prostate Imaging for Recurrence Reporting Scoring System. Radiol Clin North Am 2024;62(1):135–159.
35. Mertan FV, Greer MD, Borofsky S, et al. Multiparametric Magnetic Resonance Imaging of Recurrent Prostate Cancer. Top Magn Reson Imaging 2016;25(3):139–147.
36. Gaur S, Turkbey B. Prostate MR Imaging for Posttreatment Evaluation and Recurrence. Radiol Clin North Am 2018;56(2):263–275.
37. Sella T, Schwartz LH, Hricak H. Retained seminal vesicles after radical prostatectomy: frequency, MRI characteristics, and clinical relevance. AJR Am J Roentgenol 2006;186(2):539–546.
38. Allen SD, Thompson A, Sohaib SA. The normal post-surgical anatomy of the male pelvis following radical prostatectomy as assessed by magnetic resonance imaging. Eur Radiol 2008;18(6):1281–1291.
39. Potretzke TA, Froemming AT, Gupta RT. Post-treatment prostate MRI. Abdom Radiol (NY) 2020;45(7):2184–2197.
40. Tanaka T, Yang M, Froemming AT, et al. Current Imaging Techniques for and Imaging Spectrum of Prostate Cancer Recurrence and Metastasis: A Pictorial Review. RadioGraphics 2020;40(3):709–726.
41. Valle LF, Greer MD, Shih JH, et al. Multiparametric MRI for the detection of local recurrence of prostate cancer in the setting of biochemical recurrence after low dose rate brachytherapy. Diagn Interv Radiol 2018;24(1):46–53.
42. Gelikman DG, Mena E, Lindenberg L, et al. Reducing False-Positives Due to Urinary Stagnation in the Prostatic Urethra on 18 F-DCFPyL PSMA PET/CT With MRI. Clin Nucl Med 2024;49(7):630–636.
43. Yoshida K, Takahashi N, Karnes RJ, Froemming AT. Prostatic Remnant After Prostatectomy: MR Findings and Prevalence in Clinical Practice. AJR Am J Roentgenol 2020;214(1):W37–W43.
44. Vargas HA, Wassberg C, Akin O, Hricak H. MR imaging of treated prostate cancer. Radiology 2012;262(1):26–42.
45. Mazaheri Y, Vargas HA, Nyman G, Akin O, Hricak H. Image artifacts on prostate diffusion-weighted magnetic resonance imaging: trade-offs at 1.5 Tesla and 3.0 Tesla. Acad Radiol 2013;20(8):1041–1047.
46. Schenck JF. The role of magnetic susceptibility in magnetic resonance imaging: MRI magnetic compatibility of the first and second kinds. Med Phys 1996;23(6):815–850.
47. Wang Y, Truong TN, Yen C, et al. Quantitative evaluation of susceptibility and shielding effects of nitinol, platinum, cobalt-alloy, and stainless steel stents. Magn Reson Med 2003;49(5):972–976.
48. Tamada T, Sone T, Jo Y, et al. Locally recurrent prostate cancer after high-dose-rate brachytherapy: the value of diffusion-weighted imaging, dynamic contrast-enhanced MRI, and T2-weighted imaging in localizing tumors. AJR Am J Roentgenol 2011;197(2):408–414.
49. Connor MJ, Gorin MA, Ahmed HU, Nigam R. Focal therapy for localized prostate cancer in the era of routine multi-parametric MRI. Prostate Cancer Prostatic Dis 2020;23(2):232–243.
50. Heard JR, Naser-Tavakolian A, Nazmifar M, Ahdoot M. Focal prostate cancer therapy in the era of multiparametric MRI: a review of options and outcomes. Prostate Cancer Prostatic Dis 2023;26(2):218–227.
51. Giganti F, Dickinson L, Orczyk C, et al. Prostate Imaging after Focal Ablation (PI-FAB): A Proposal for a Scoring System for Multiparametric MRI of the Prostate After Focal Therapy. Eur Urol Oncol 2023;6(6):629–634.
52. Gelikman DG, Kenigsberg AP, Yilmaz EC, et al. Evaluating diagnostic accuracy of the Prostate Imaging after Focal Ablation (PI-FAB) scoring system in detecting clinically significant prostate cancer after primary focal therapy. J Clin Oncol 2024;42(4 suppl):277.
53. Gelikman DG, Kenigsberg AP, Mee Law Y, et al. Evaluating Diagnostic Accuracy and Inter-reader Agreement of the Prostate Imaging After Focal Ablation Scoring System. Eur Urol Open Sci 2024;62:74–80.
54. Light A, Mayor N, Cullen E, et al. The Transatlantic Recommendations for Prostate Gland Evaluation with Magnetic Resonance Imaging After Focal Therapy (TARGET): A Systematic Review and International Consensus Recommendations. Eur Urol 2024;85(5):466–482.
55. Gold SA, VanderWeele DJ, Harmon S, et al. mpMRI preoperative staging in men treated with antiandrogen and androgen deprivation therapy before robotic prostatectomy. Urol Oncol 2019;37(6):352.e25–352.e30.
56. Chen Z, Zhou B, Liu W, et al. Diagnostic efficacy and interobserver agreement among readers with variable experience of the Prostate Imaging for Recurrence Reporting system with whole-mount histology after androgen deprivation therapy as a reference. Quant Imaging Med Surg 2024;14(4):3006–3017.
57. Hofman MS, Hicks RJ, Maurer T, Eiber M. Prostate-specific Membrane Antigen PET: Clinical Utility in Prostate Cancer, Normal Patterns, Pearls, and Pitfalls. RadioGraphics 2018;38(1):200–217.
58. Crocerossa F, Marchioni M, Novara G, et al. Detection Rate of Prostate Specific Membrane Antigen Tracers for Positron Emission Tomography/Computerized Tomography in Prostate Cancer Biochemical Recurrence: A Systematic Review and Network Meta-Analysis. J Urol 2021;205(2):356–369 [Published correction appears in J Urol 2021;205(4):1237.].
59. Jansen BHE, Bodar YJL, Zwezerijnen GJC, et al. Pelvic lymph-node staging with ^{18}F-DCFPyL PET/CT prior to extended pelvic lymph-node dissection in primary prostate cancer: the SALT trial. Eur J Nucl Med Mol Imaging 2021;48(2):509–520.
60. Pienta KJ, Gorin MA, Rowe SP, et al. A Phase 2/3 Prospective Multicenter Study of the Diagnostic Accuracy of Prostate Specific Membrane Antigen PET/CT with ^{18}F-DCFPyL in Prostate Cancer Patients (OSPREY). J Urol 2021;206(1):52–61.
61. Tanaka T, Kawashima A, Rangel LJ, et al. Long-Term Risk of Clinical Progression Utilizing Magnetic Resonance Imaging Findings of Locally Recurrent Prostate Cancer in Patients with Biochemical Recurrence following Radical Prostatectomy. J Urol 2022;207(5):1038–1047.
62. Evangelista L, Zattoni F, Cassarino G, et al. PET/MRI in prostate cancer: a systematic review and meta-analysis. Eur J Nucl Med Mol Imaging 2021;48(3):859–873.